MODAL AND STRESS ANALYSIS OF GEAR TRAIN OF A ROTAVATOR

A

Dissertation

Submitted in partial fulfillment of the requirement for the award of degree

MASTER OF ENGINEERING

in

CAD/CAM & ROBOTICS

Submitted By

Omesh Goyal

(Roll No. 821181006)

Under Guidance of

Mr. Bikramjit Sharma
Assistant Professor
Deptt. of Mechanical Engg.
Thapar University Patiala

DEPARTMENT OF MECHANICAL ENGINEERING

THAPAR UNIVERSITY, PATIALA-147004, INDIA

(Declared as Deemed-to-be university u/s of the UGC Act, 1956)

July, 2014

Dedicated to my sister (Mukta) and jiju (Sourabh)

CERTIFICATE

This is to certify that the work done in this dissertation entitled "**MODAL AND STRESS ANALYSIS OF GEAR TRAIN OF A ROTAVATOR**" submitted in partial fulfilment of requirement for the award of Master of Engineering Degree in CAD/CAM & Robotics in Mechanical Engineering Department of Thapar University, Patiala, is an authentic record of work carried out by me under the guidance of **Mr. Bikramjit Sharma**, Assistant Professor, Mechanical Engineering Department, Thapar University, Patiala.

The matter embodied in this dissertation report has not been submitted in part or full to any university or institute for the award of any degree.

Omesh Goyal

Omesh Goyal

Dated: 10/July/2014

This is to certify that the above declaration made by the student concern is correct to the best of my knowledge and belief.

Bikramjit Sharma

Mr. Bikramjit Sharma
Assistant Professor
Deptt. Of Mechanical Engg.
Thapar University, Patiala.

Countersigned By:

Dr. Ajay Batish
Professor & H.M.E.D.
Thapar University, Patiala.

Dr. S.K. Mohapatra
Dean Academics Affairs
Thapar University, Patiala.

ACKNOWLEDGEMENT

I am highly grateful to the authorities of Thapar University, Patiala for providing this opportunity to carry out the dissertation work.

I would like to express a deep sense of gratitude and thank profusely to my dissertation supervisor **Mr. Bikramjit Sharma**, Assistant Professor, Mechanical Engineering Department, Thapar University, Patiala. for his sincere & invaluable guidance and suggestions which inspired me to submit dissertation in the present form.

Omesh Goyal

ABSTRACT

Rotavator is one of the tillage machine which is used in arable field preparing the seedbed preparation directly. Rotavator is attached to three point linkage system of a tractor and it is driven by the tractor power take off (PTO). Rotavator construction has a gear box that changes motion direction with 90° from tractor PTO, transmission gears for rotation velocity and a rotor shaft which placed as horizontal to soil for blending. In this work transmission gear train of a rotavator is analyzed considering bending stresses, contact stresses and mode shapes. The effect of reducing thickness of web in gears is also studied. The reduced thickness of web resulted in redistribution of stresses and led to decrease in magnitude of localized stresses. Simple design modifications, reducing the thickness of web of gears are also implemented after successful validation of finite element solution.

TABLE OF CONTENT

LIST OF FIGURES

LIST OF TABLES

1.1 Rotavator

Rotavator is one of the culturing instruments which gets motion from tractor power take off (PTO) and it had been designed for mix to soil. Soil traffic is decreased to incredible degree with this tool by mixing the soil. Rotavator construction has a gear box that alter motion direction with 90 degrees from tractor PTO, transmission gears for rotation velocity and a rotor shaft which is put as horizontal to soil for blending. There are cutter blades on rotor shaft for breaking into pieces and mic to soil. Especially, on cutter blade and transmission gears, deformations occur because of high vibration, pointless high power, impact effect of soil parts, design manufacturing error and wrong usage conditions. Especially for transmission parts, study of stresses is important to understand failure reasons. In this study, transmission gear train of a rotavator which was designed and manufactured by a local manufacturer is analyzed.

Fig. 1.1 Rotavator attached to the tractor [23]

Fig. 1.2 Transmission system of the rotavator [23]

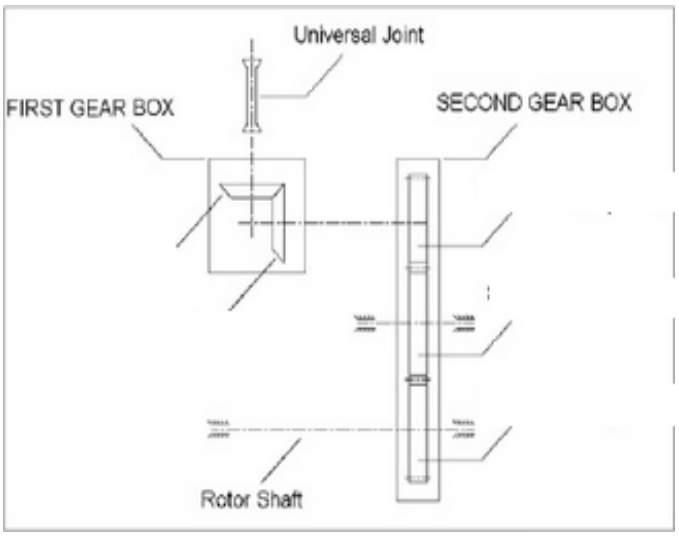

Fig. 1.3 Transmission scheme of the rotavator [23]

1.2 Introduction of gears

Gearing is one of the most critical parts in a mechanical power transmission framework, and in most industrial rotating machinery. A gearbox is normally utilized in the transmission system is also called a speed reducer, gear head, gear reducer etc., which consists of a set of gears, shafts and bearings that are factory mounted in an enclosed lubricated housing. Speed reducers are available in a broad range of sizes, capacities and speed ratios. Their job is to convert the input provided by a prime mover (usually an electric motor) into an output with lower speed and correspondingly higher torque.

The expanding interest for quiet power transmission in machines, vehicles, lifts and generators, has made a developing interest for a more precise analysis of the characteristics of gear systems. In the automobile industry, the largest manufacturer of gears, higher reliability and lighter weight gears are necessary as lighter automobiles continue to be in demand.

1.3 Law of gearing

A essential requirement of gears is the consistency of angular velocities or proportionality of position transmission. Rapid and/or high-power gear trains also require transmission at constant angular velocities in order to avoid problems. Constant velocity (i.e., constant ratio) motion transmission is defined as "conjugate action" of the gear tooth profiles. A geometric relationship might be determined for the form of the tooth profiles to provide conjugate action, which is summarized as the Law of gearing as follows:

"A typical ordinary to the tooth profiles at their point of contact must, in all positions of the contacting teeth, pass through a fixed point on the line-of-centers called the pitch point." Any two curves or profiles engaging each other and satisfying the law of gearing are conjugate curves.

Fig. 1.4 shows two mating gear teeth, in which

• Tooth profile 1 drives tooth profile 2 by acting at the instantaneous contact point K.

• N_1 N_2: common normal of the two profiles.

• N_1: foot of the perpendicular from O_1 to N_1N_2

• N_2: foot of the perpendicular from O_2 to N_1N_2.

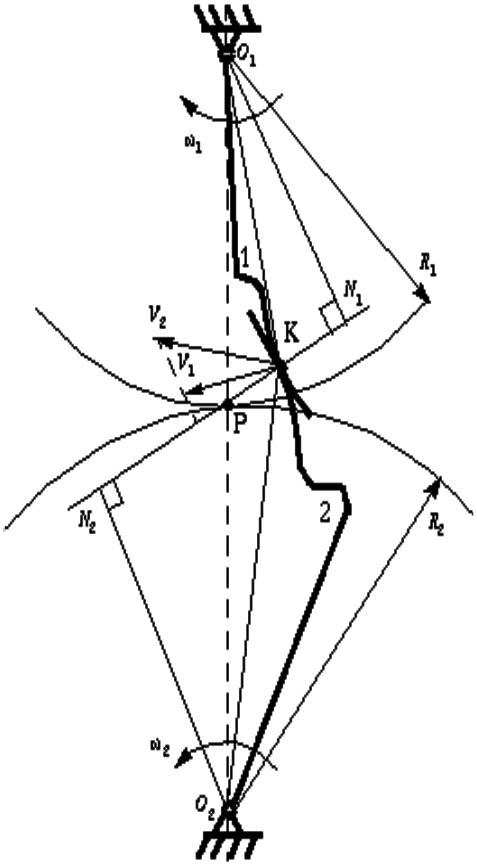

Fig. 1.4 Law of gearing [23]

Although the two profiles have different velocities V_1 and V_2 at point K, their velocities along N_1N_2 are equal in both magnitude and direction. Otherwise the two tooth profiles would separate from each other. Therefore,

$$O_1 N_1 . \omega_1 = O_2 N_2 . \omega_2$$

Or

$$\frac{\omega_1}{\omega_2} = \frac{O_2 N_2}{O_1 N_1}$$

It is noticed that the intersection of the tangency N_1N_2 and the line of center O_1O_2 is at point P, and

$$O_1 N_1 . \omega_1 = O_2 N_2 . \omega_2$$

Thus, the relationship between the angular velocities of the driving gear to the driven gear, or velocity ratio, of a pair of mating teeth is

$$\frac{\omega_1}{\omega_2} = \frac{O_2 P}{O_1 P}$$

Point P is very important to the velocity ratio, and it is called the pitch point. Pitch point divides the line between the line of centers and its position decides the velocity ratio of the two teeth. The above expression is the fundamental law of gear-tooth action.

1.4 Conjugate action

Mating gear teeth acting against one other to create rotating movements are like cams. When the tooth profiles, or cams, are designed so as to produce a constant angular-velocity ratio during meshing, these are said to have conjugate activity. In theoretical, at least, it is possible arbitrarily to choose any profile for one tooth and afterward to discover a profile for the meshing tooth which will give conjugate action. One of these results is the involute profile, with few exceptions it is in universal use for gear teeth.

There are two forms of tooth profile commonly used:-

i. Cycloidal teeth
ii. Involute teeth

Cycloidal teeth

An advantage of the cycloidal teeth over the involute one is that wear of cycloidal tooth is not as fast as with involute tooth. For this reason, gears transmitting very large amount of power are sometimes cut with cycloidal teeth. On the other hand, involute teeth are very easy to manufacture and the actual distance between the centers may deviate slightly from the theoretical distance without affecting the velocity ratio or general performance, because of this distinct advantage, gears with involute cut teeth are used much more than those with cycloidal teeth.

Involute properties

There are almost an infinite number of curves that can be developed to satisfy the law of gearing, and many different curve forms have been tried in the past. Modern gearing (except for clock gears) is based on involute teeth. This is due to three major advantages of the involute curve:

i. Conjugate action is independent of changes in center distance.
ii. The form of the basic rack tooth is straight-sided, and therefore is relatively simple and can be accurately made; as a generating tool it imparts high accuracy to the cut gear tooth.

iii. One cutter can generate all gear teeth numbers of the same pitch.

An involute may be created as demonstrated in fig. 1.5 a partial flange B is joined to the cylinder A, around which is wrapped a cord *def* which is held tight. Point b on the cord represents the tracing point, and as the cord is wrapped and unwrapped about the cylinder, point b will trace out the involute curve ac.

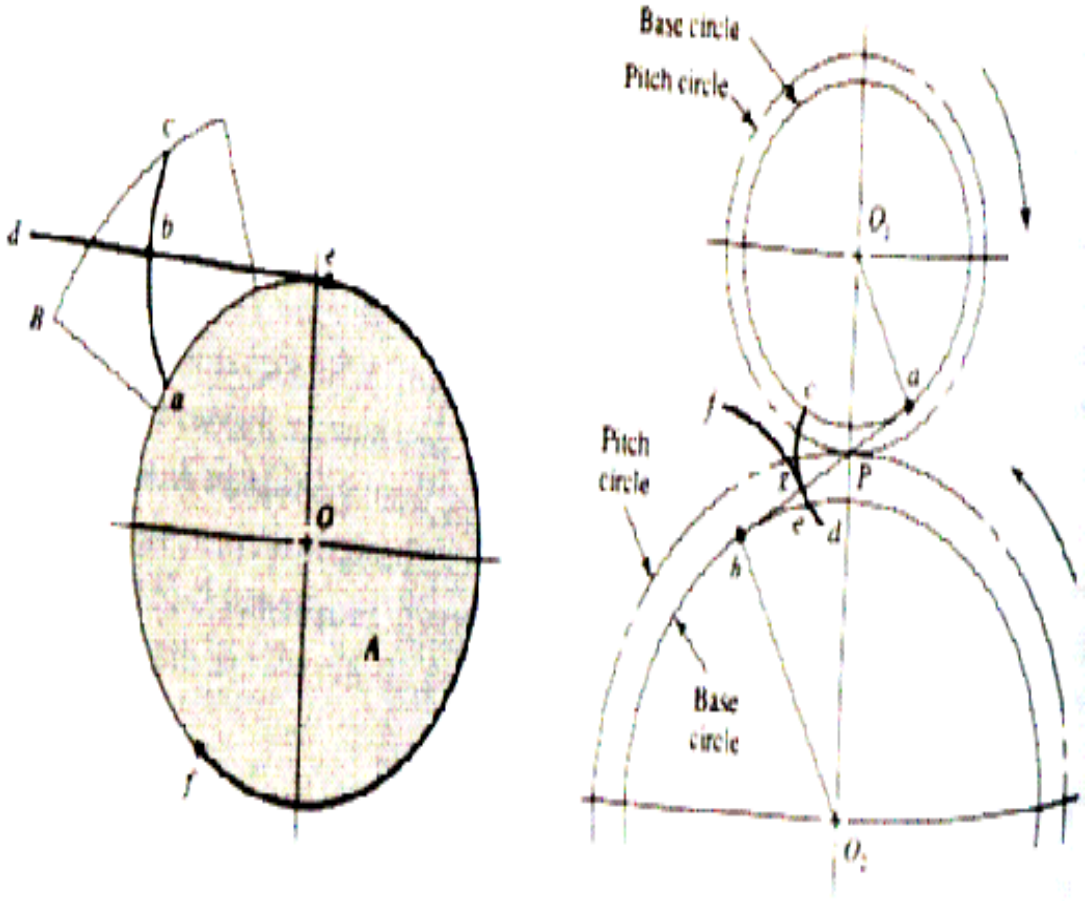

Fig. 1.5 Generation of an involute and involute action [23]

The radius of the curvature of the involute changes continuously, being zero at point 'a' and a maximum at point c. at point b the radius is equal to the distance be, since point "be" is rotating about point e. Thus generating line "de" is normal to the involute at all point of intersection and at the same time, is always tangent to the cylinder A. The circle on which the involute is generated is called the base circle.

1.5 Gear nomenclature

The following terms are universally used in gears terminology (refer fig. 1.6).

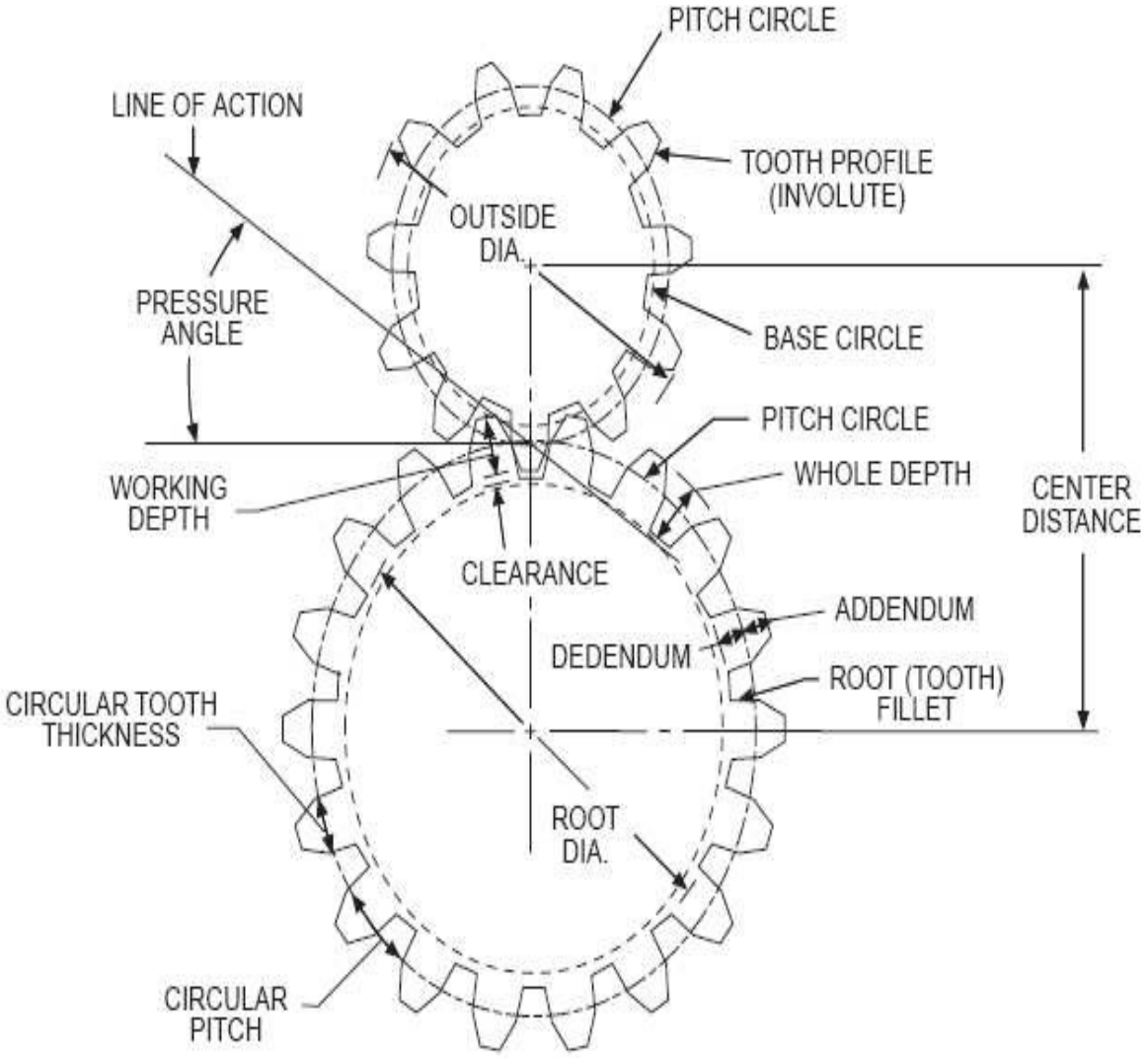

Fig. 1.6 Gear nomenclature [23]

ADDENDUM (a) is the height by which a tooth ventures beyond the pitch circle or pitch line.

BASE DIAMETER (D_b) is the width of the base cyclinder from which the involute portion of a tooth profile is produced.

BACKLASH (B) is the amount by which the width of a tooth space exceeds the thickness of the engaging tooth on the pitch circles. As actually indicated by measuring devices, backlash may be determined variously in the transverse, normal, or axial-planes, and either in the direction of the pitch circles or on the line of action. Such measurements should be corrected to corresponding values on transverse pitch circles for general comparisons.

BORE LENGTH is the total length through gear, sprocket, or coupling bore.

CIRCULAR PITCH (p) is the length of the arc of the pitch circle between similar faces of successive teeth.

CIRCULAR TOOTH THICKNESS (t) is the length of arc of pitch circle between opposite faces of the same tooth.

CLEARANCE-OPERATING (c) it is difference between the addendum of a gear and the dedendum of its mating gear .

CONTACT RATIO (m_c) the number of angular pitches through which a tooth surface rotates from the beginning to the end of contact.

DEDENDUM (b) is the depth of a tooth space below the pitch circle. It is equal to addendum plus clearance.

DIAMETRAL PITCH (P) is the number of teeth divided by the pitch diameter.

FACE WIDTH (F) is the length of the tooth in axial plane.

FILLET RADIUS (r_f) is the rounded corner at the base of the gear tooth.

FULL DEPTH TEETH are those in which the working depth equals 2 to the normal diametrical pitch.

HUB DIAMETER is outside diameter of a gear, sprocket or coupling hub.

HUB PROJECTION is the distance the hub extends beyond the gear face.

INVOLUTE TEETH of spur gears, helical gears and worms are those in which the active portion of the profile in the transverse plane is the involute of a circle.

LONG- AND SHORT-ADDENDUM TEETH are engaging gears one of which has a long addendum and the other has a short addendum.

KEYWAY is the machined groove running the length of the bore. A similar groove is machined in the shaft and a key fits into this opening.

OUTSIDE DIAMETER (D_o) is the diameter of the addendum (outside) circle.

PITCH CIRCLE is the circle derived from a number of teeth and a specified circular pitch.

Circle on which spacing or tooth profiles is established and from which the tooth proportions are constructed.

PITCH CYLINDER is the cylinder of diameter equal to the pitch circle.

PINION is a machine part with gear teeth. When two gears run together, the one with the smaller number of teeth is called the pinion.

PITCH DIAMETER (D) is the diameter of the pitch circle. In parallel shaft gears, the pitch diameters can be determined directly from the center distance and the number of teeth.

PRESSURE ANGLE (ø) it is the acute angle formed between the line of action and common tangent to the two pitch circles, which passes through the pitch point.

ROOT DIAMETER (D_r) is the diameter at the bottom of the tooth space.

PRESSURE ANGLE-OPERATING ($ø_r$) is determined by the center distance at which the gears operate. It is the pressure angle at the operating pitch diameter.

TIP RELIEF is an arbitrary modification of a tooth profile whereby a small amount of material is removed near the tip of the gear tooth.

UNDERCUT is a condition in generated gear teeth when any part of the fillet curve lies inside a line drawn tangent to the working profile at its point of juncture with the fillet.

WHOLE DEPTH (h_t) it is sum of the addendum and dedendum of a tooth.

WORKING DEPTH (h_k) is the distance by which a tooth extend in to the space of a mating gear and it is equal to whole depth minus the clearance, or twice the addendum.

1.6 Analysis of stresses

The analysis of stresses can be done by analytical method or by approximate method, like finite element analysis, gentic algorithms, other computer programs. These analysis are based on determining bending stresses and contact stresses.

1.6.1 Bending and contact stress in gear tooth

There are two kinds of stresses in gear teeth, root bending stresses and tooth contact stresses. These two stresses results in the failure of gear teeth, root bending stress results in fatigue fracture and contact stresses results in pitting failure at the contact surface. So both these stresses are to be considered when designing gears.

AGMA bending stress of gear tooth

Bending stress on a gear tooth is mainly resulted from the tangential force components acting on the tooth. Based on this, Lewis derived the equation to determine the bending stress on a gear tooth. Assuming gear tooth as a cantilever beam and the entire load to be transmitted through one tooth, an equation for the bending stress is as follows.

$$\sigma = \frac{W_t P_d}{b.Y} \tag{1.1}$$

Where

- W_t is Tangential load acting on the gear tooth
- P_d is Diametrical Pitch of Gear
- Y is Lewis Form Factor
- σ is Bending Stress
- b is Face Width

In the above equation stress concentration at tooth fillet is not considered, so AGMA derived a new bending stress equation by introducing stress concentration factor to reduce the impact of stresses near tooth fillet which is given by

$$\sigma = \frac{W_t.P_d.K_t}{bY} \tag{1.2}$$

Where

- K_t is Stress concentration factor

For Practical design considerations AGMA suggests more design factors to estimate bending stress on gear tooth. The modified bending stress is given by the following equation

$$\sigma_s = \frac{W_t P_d}{b.J} K_0 K_v K_m K_s K_B \quad (1.3)$$

Where

- K_o: Overload factor
- K_v: is Dynamic factor
- K_m: Load distribution factor
- K_s: Size distribution factor
- K_B: is Rim thickness factor

The definitions of these factors are presented in the following section

Definition of AGMA bending stress factors

Overload factor (K_o)

This factor represents the behavior of the gear on application of the external loads. These factors mainly include the vibrations, shocks, speed variations and other specific loading conditions.

Dynamic factor (K_v)

Dynamic Factor mainly depends on the tooth profile inaccuracies, speed of approach of tooth, vibrations of tooth during meshing, tooth friction, Dynamic imbalance of rotating members, and Gear shaft misalignment and elastic property of the tooth. Dynamic factor is generally given by the following formula

$$K_v = \left(\frac{A+\sqrt{V}}{A}\right)^B \quad (1.4)$$

$$(V_t)_{max} = [A + (Q_v - 3)]^2 \quad (1.5)$$

Where

- A is 50+56(1-B),
- B = $0.25(12-Q_v)^{2/3}$
- Q_v is Transmission accuracy level
- V_t is Pitch line velocity

Load distribution factor (K_m)

Determination of load distribution factor depends on various factors which include the design of gear as well as design of shaft, bearings, housing and structure on which gear drive is mounted. The main objective of the load distribution factor is to reflect the non-uniform load

distribution across the line of contact. The load distribution factor can either be defined by AGMA 2001/2101 or can be defined directly which is given by

$$K_m = 1 + C_{pf} + C_{ma} \quad (1.6)$$

Where

- C_{pf} is Proportion Factor
- C_{ma} is Mesh alignment Factor

Size distribution factor

Size Distribution factors resonates the material non-uniform properties due to its size. The main factors include

- Tooth size
- Part diameter
- Tooth size to diameter of part
- Face width
- Area of stress pattern

However AGMA suggests the value of Ks to be 1 for diametrical pitch greater than or equal to 5 and following table suggests the size factor for diametrical pitches less than 5.

Rim thickness factor

The Lewis Equation assumes gear tooth as a cantilever beams attached perfectly to a rigid base. If the rim is thin, it deforms and causes the point of maximum stress to shift from fillet to some point on the rim. This factor estimates the influence of stress on the rim which is given by

$$K_B = \{1.6Ln\frac{2.242}{m_b}\ ;\ m_b < 1.2 \quad (1.7)$$

$$1;\ m_b \geq 1.2$$

Where

- m_b is equal to t_r / h_r.
- t_r is Rim thickness below the tooth.
- h_r is tooth height.

Hertz contact stress

Contact stress

Pitting is a surface fatigue failure resulting because of redundancies of high contact stress. When loads are applied to bodies, their surfaces distort elastically close to the point of contact; so that a small area of contact is deformed. It is accepted that, as this small area

of contact forms, points that come into contact are points on the two surfaces that originally were equal distances from the tangent plane. Pitting generally occurs on operating surfaces of gear teeth, a basic cause is excessive loading that increased contact stresses beyond critical levels. In it we will define contact stress according to Hertz contact stress equation. The Hertz theory assumes an elliptic stress distribution. The maximum stress is in the middle and equals

$$\sigma_{\text{Hertz}} = \sqrt{\frac{W(\frac{1}{R_1}+\frac{1}{R_2})}{b\pi[\frac{1-\mu_1^2}{E_1}+\frac{1-\mu_2^2}{E_2}]}} \tag{1.8}$$

Where

- W : Normal Load
- E_1, E_2 : Elastic modulus of pinion and gear
- b : Face width
- μ_1, μ_2 : Poission ratio of pinion and gear
- R_1, R_2 : Raddi at the contact point of the involute curve
- $R_1 = r_{b1}.\sin\emptyset$, $R_2 = r_{b2}.\sin\emptyset$
- r_{b1}, r_{b2} = pitch circle radius of pinion and gear respectively

Hence the Hertzian equation become

$$\sigma_{Hertz} = \sqrt{\frac{W(1+\frac{r_{b1}}{r_{b2}})}{b\pi r_{b1}[\frac{1-\mu_1^2}{E_1}+\frac{1-\mu_2^2}{E_2}]sin\emptyset}} \tag{1.9}$$

1.6.2 Stress analysis using finite element analysis

Finite element method

The finite Element Method has become a very powerful tool for the numerical solution of a wide range of application. The application ranges from deformation and stress analysis of automotive parts, aircraft, building and bridge structures etc. Finite element method not only gives the behavioral insight of the different part of the structure but it also analyzes the structure taking the individual behavior of these parts consideration

Basic steps of finite element analysis

Pre processing	• Geometry formulation • Type of analysis • Material properties • Element type • Discretization • Loads and boundary conditions • Model display
Solution	• Run analysis to obtain solution (stresses & displacements)
Post processing	• Graphical display of stresses and displacements for quick and easy interpretation of results.

1.7 Types of gear tooth failures

The gears generally fail when tooth stress exceeds the safe limit. When failure occurs, they are expensive not only in terms of the cost of replacement or repair but also the cost associated with the downtime of the system of which they are a part. So, it is important to understand various problems that can occur in gears. The types of gear tooth failure can be categorized into following classes:

- Wear
- Scoring
- Interference
- Surface fatigue
- Plastic Flow
- Fracture
- Process Related

Wear

Wear occurs when the film of lubricant that exists between the mating surfaces of the teeth is not sufficient to counteract surface-to-surface contact. Different variables in charge of wear, for example abrasive particles in the lubricant, corrosion of tooth surfaces, aberrations in the tooth surfaces themselves that penetrate the lubricant film, relative surface roughness of the tooth flanks, and the amount of contamination in the lubricant depending on the extent and the cause of wear, it can be of following types:

- Polishing wear
- Moderate wear
- Excessive wear
- Abrasive wear
- Corrosive wear

Scoring

Scoring is generally observed on high-speed, high-load gearing. Most often these gears are operating with low-viscosity, synthetic lubricants. If the combination of load, sliding velocity, and inlet oil temperature reaches a critical value, the oil film separating the mating surfaces is destroyed, and metal-to-metal contact occurs. If the surface pressure and sliding velocity are high enough, instantaneous welding of the asperities will then occur. As the gears continue to rotate, the welds break. This phenomenon is known as scoring. Depending on the extent and the cause of scoring, it can be of following types:

- Frosting
- Light Scoring
- Moderate Scoring
- Destructive Scoring
- Localized Scoring

Interference

Interference of one tooth with another, can effect on the operation of the system. A wide variety of conditions, such as operating on tight centers, insufficient involute, thermal expansion, misalignment and insufficient or incorrect profile modifications can cause interference. Depending on the region or interference, it can be of following types:

- Tip interference
- Root interference

Surface fatigue

Surface fatigue is a time-dependent phenomenon; thus its effects may not be apparent for a considerable period of time. The surface of a gear tooth is subjected to varying load. This condition is referred to as fatigue. When the fatigue capacity of the material is exceeded, it will fail. It generates substantial quantities of chips in their later stages of progression. Depending on the extent of surface fatigue, it can be of following types:

- Initial pitting
- Destructive pitting
- Spalling
- Case crushing

Plastic flow

Plastic flow does progress with time and can ultimately be catastrophic. It is not strictly a fatigue phenomenon. Very heavy loads, usually combined with relatively slow speed rotation can cause gear materials to flow plastically.

Depending on the specific conditions encountered, plastic flow may take any of several forms:

- Cold flow
- Hot flow
- Rippling
- Ridging

Fracture

Fracture is a much more insidious type of failure. It produces no debris in its early stages, gives little warning, and usually results in either immediate loss of serviceability or greatly reduced power transmitting capacity. All the failure modes discussed above are progressive, i.e the time between failure initiation & complete loss of serviceability is frequently quite long. This is of particular importance in the design of devices such as helicopters, elevators, cranes, and so forth in which a complete failure to transmit rotation may result in human

injury or death. For these reasons, gears are generally designed with a larger maintain or safety when considering the fracture modes. Depending on the way in which the fracture occurs, it can be of following types:

- Classical bending fatigue
- Over load
- Random fracture
- Root/Rim/Web
- Resonance

Process related

There are many types of failures that occur even before the gears placed in service. The very best design, on paper, can be a total disaster if it is not faithfully executed in the manufacturing phase. Process Related failure can be of following types:

- Quench cracks, Grinding cracks
- Grinding cracks
- Nicks, scratches
- Electric arching
- Grinding “Burns”
- Improper edge breaks and tool marks

Ooi et al. (2012) performed a modal and stress analysis on a gear train of portal axle unit with a FEA software. Modal analysis was performed under free-stress and pre-stress conditions. Results obtained from stress analysis were validated with results obtained from Lewis hypothesis and Hertz hypothesis. Both bending and contact stress were in good concurrence with the difference of 4% to 6 % . Besides, the input gear had overall higher bending stress compared to the bending stress at the output gear. When gear train was analyzed under varying angular positions, the bending and contact stress results were not consistent when plotted against the angular position. This was because of irregularities and low surface smoothness in the geometrical mesh model.

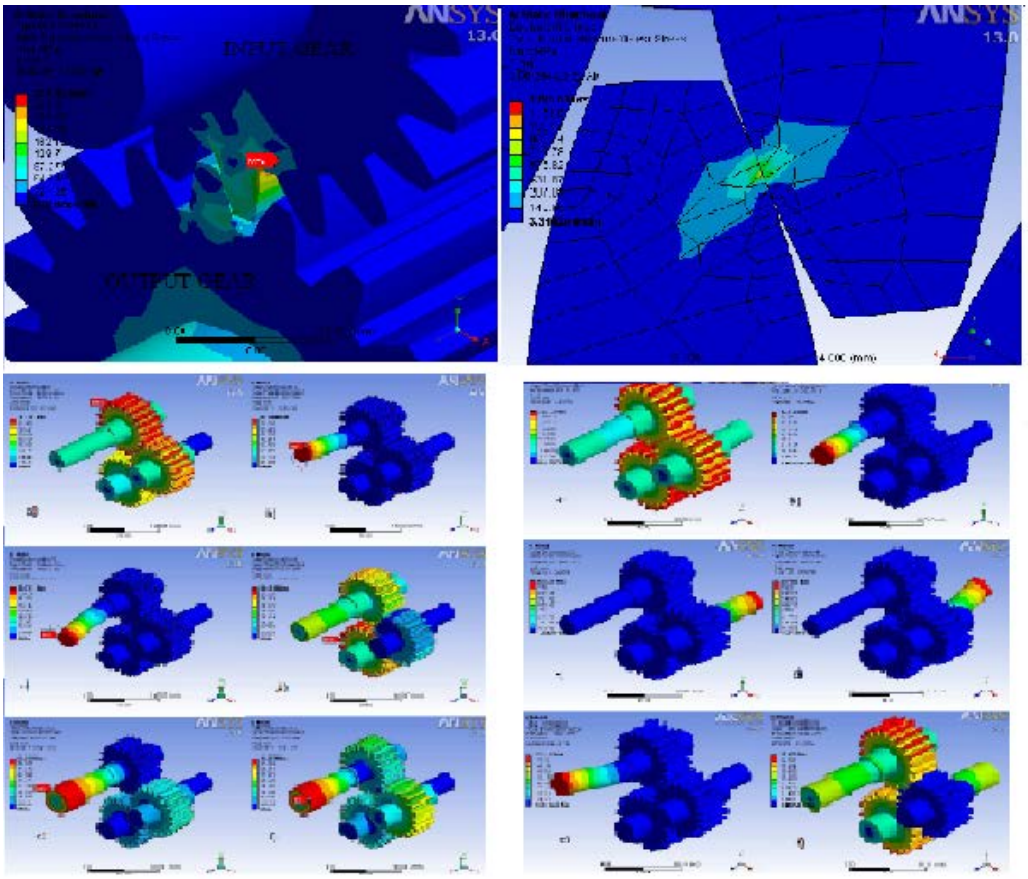

Fig. 2.1 Results of bending, contact stresses and mode shapes [1]

Topakci et al. (2008) simulated stress distributions on transmission gears of a rotary tiller. The transmission gears were modeled using Solidworks 3D parametric software and structural stress analysis was performed on Cosmos works finite elements software. When transmission gears was evaluated in simulation software no failure was occur, and gears were

working well. From this they conclude that designers used the material for manufacturing of gear which had high coefficient of safety but in this way cost of material increased.

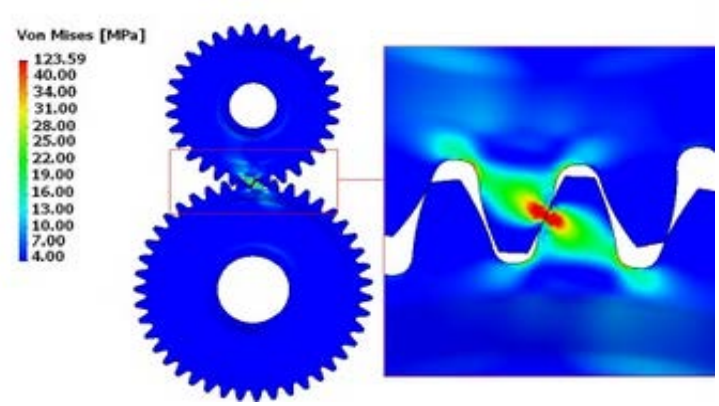

Fig. 2.2 Result of contact stress [2]

Hassan (2009) presented the study which deals with contact stresses of gears considering contact ratio, approach angle, recess angle, length of contact. To apply finite element method in contact stress a special technique was used rather the regular elements, to distinguish between the contact regions which were in two parts. One was the first body named target region and the other body was named contact region. For target region, target elements were used and in contact region contact elements were used. ANSYS software presented a significant technique for this purpose which was used here. A computer program was developed to plot one pair of teeth in contact at different positions of contact depending on the formulation. The selected angular interval value was 3°, the progress of contact was studied at each 3° interval, which means that there were 10 cases of contact under consideration. These 10 cases were used to build 10 finite element contact models and contact finite element analysis was done under the load and material conditions were named. The maximum stress result obtained from AGMA stress calculation method was 587MPa while the maximum contact stress obtained from the finite element contact analysis was 595MPa (case five) under the same conditions, it was clear that the agreement was good.

Patel et al. (2010) developed a three dimensional deformable-body model of spur and helical gear. Modeling was done using relational equation in Pro-engineer, then bending and contact stresses were obtained using Ansys FEM package software and results obtained were then compared with the AGMA theoretical stress values. The results were good congruence with the theoretical values, which implies that the model designed was correct. This process can be very helpful in contact problems as it needs model with high accuracy. It also decreased the lead times. The Finite Element results matched well with the numerical results. Thus this

parametric model turns out to be a fast and accurate method of computing stress problem of the involute tooth gear system.

Li (2007) presented a three-dimensional, finite element model considering contact stress and root bending stress and performed calculations for a pair of spur gears with machining errors, assembly errors and tooth modifications. The responsive FEM programs were developed based on the presented methods. Tooth contact lengths of a pair of spur gears with lead crowning were calculated by the programs and compared with measured ones. Tooth contact pattern and root stains of a pair of spur gears with assembly errors were also calculated by the programs and compared with experimental results. It was found that machining errors, assembly errors and tooth modifications exert great effects on tooth contact stress and bending stress. Especially, when the effects of machining errors, assembly errors and tooth modifications were considered together at the same time, surface contact stress and root bending stress become much greater than the case without errors and tooth modifications. Surface contact stress and root bending stress of the same pair of spur gears were also calculated by ISO standards for comparing with the FEM results, so FEM programs developed can be used as a tool to do precise analyses of surface contact stress and root bending stress of a pair of spur gears with machining errors, assembly errors and tooth modifications.

Perez et al. (2011) Implemented an approach based on the Hertz theory for determination of contact variables, such as the contact area, the pressure distribution, the maximum contact pressure, and the stress distribution underneath the contacting surfaces. The maximum tresca stress, and the compression, for gear drives with localized bearing contact at edge contact was avoided by whole crowning of the tooth surfaces. A finite element model had been developed and validated in terms of the contact area, the maximum contact pressure, the pressure distribution along major and minor semi-axes of the contact area and the principal stress distribution underneath the contacting surfaces.

Li (2008) investigated the **e**ffect of addendum on contact strength, bending strength and basic performance parameters of two pairs of spur gears through performing exact finite element analyses of the spur gears with different addendums and high contact ratios. In order to perform precise analyses, a face-contact model, mathematical programming method and three-dimensional, finite element method were used together to conduct loaded tooth contact analyses, deformation and stress calculations of the spur gears. Tooth load distributions, load sharing-rate, surface contact stresses, root bending stresses, transmission errors and mesh

stiffness of a pair of gears with non-standard addendum were analyzed. This study revealed that Hertz formula was not exact enough for the contact stress calculation of a pair of gears in the engagement position far away from the pitch point. Also hertz formula cannot be used for contact stress calculation of the gears at tip or root contact. If changed addendum did not increase number of contact teeth, then tooth load-sharing rate should be changed slightly. Tooth load-sharing rate can be changed greatly if the number of contact teeth increased through increasing addendum. Tooth root stress increased if addendum becomes longer and number of contact teeth had no change. Tooth root stress can also be reduced when the number of contact teeth increased through increasing the addendum. Tooth contact stress and contact width were changed slightly if addendum becomes longer and number of contact teeth not changed. But they reduced greatly if the number of contact teeth increased through increasing the addendum. Transmission error of the gears increased if addendum becomes longer and number of contact teeth not changed. But it can also be reduced by increasing the number of contact teeth. Mesh stiffness reduced if addendum becomes longer and number of contact teeth not changed. But it can also be increased by increasing the number of contact teeth.

Chen et al. (2013) developed a general analytical mesh stiffness model to consider the effect of tooth errors which may be resulted from the manufacturing errors, assembly errors and tooth profile modifications (TPM) or profile defects. The loaded transmission errors can be optimized with proper selection of tooth profile modifications and its minimum fluctuating amplitude could be obtained with sacrifice of some load carrying capacity, Under the condition with absence of corner contact, a spur gear pair with bigger amount of TPM will require a shorter length of TPM to achieve the minimized transmission error fluctuation and vice versa. Also, to achieve the minimum transmission error fluctuation with bigger load needs greater amount or longer length of TPM. The presence of the tooth root crack could reduce the amplitude of the mesh stiffness, and extend the double- or triple-tooth engagement zones of gear pairs with LCR(low contact ratio) and HCR(high contact ratio) respectively, and even cause corner contact which will devastate the dynamic performance of the gear pairs.

Sánchez et al. (2013) used a model of non-uniform load distribution along the line of contact of spur and helical gear teeth, obtained from the minimum elastic potential energy criterion, for the determination of the critical tooth-root stress, whose value was determinant for evaluating the load capacity of the gear set. The study had been restricted to gears with transverse contact ratio between 1 and 2, with non-undercut teeth. For spur gears, the critical

fatigue tooth-root stress arises with the tooth loaded with the total load at the outer point of single pair tooth contact. For helical gears, the critical fatigue bending stress could be calculated assuming that conditions of maximum of function $\Psi(\xi)$and minimum of function $Iv(\xi_0)$ were given simultaneously at some contact position. It was demonstrated that induced error was small, and in the sense of safety, if coincidence did not occur. The location of the maximum of function $\Psi(\xi)$can be computed, while the minimum of $Iv(\xi_0)$ was always located at the inner point of contact of the pinion. Equations were given for all the parameters and functions, allowing simple, analytic calculations of the tooth-root stress. Accuracy of all these calculations had been checked, and according to the obtained results was good enough for strength models.

Kramberger et al. (2004) presented a computational model for the determination of service life of gears in bending fatigue in a gear tooth root. On the basis of presented analyses, the number of loading cycles required for damage initiation (Ni) and number of loading cycles for fatigue crack propagation (Np) in the most critical region for bending fatigue have been predicted. The model enabled the user to determine the whole service life, given adequate fatigue material parameters. The crack initiation period was based on a stress–strain analysis using the FEM, where it was assumed that the crack was initiated at the point of maximum principal stress in a gear tooth root. Gear tooth crack propagation was simulated using FEM with principles of linear elastic fracture mechanics. The displacement correlation method was used for numerical determination of the functional relationship between the stress intensity factor and crack length which was necessary for consequent analysis of fatigue crack growth. The model was used to determine the complete service life of a spur gear made from high strength alloy steel 42CrMo4 (through-hardened). At low stress levels near the fatigue limit almost all service life was spent in crack initiation. This was a very important factor in determining the service life of real gears in practice, because most operate with loading conditions close to the fatigue limit.

Mao (2007) used a non-linear finite element method to accurately simulate gear contact behaviour. The models used true three dimensional gear tooth profiles with micro-geometry modifications under real load conditions. The shaft misalignment, deflection and assembly deflection effects on gear surface contact behaviour had been investigated. The optimised micro-geometry based on the analysis had been proposed to reduce surface contact fatigue failure. The model had been very successfully applied in automotive transmission gear surface fatigue wear reduction. The highly accurate gear micro-geometry modification

method had improved the gear surface fatigue wear significantly. This method can also be applied to transmission system noise analysis in term of transmission error reduction.

Hedlund et al. (2007) performed analysis of helical gear contact problem in which helical gear surface profiles were constructed from gear tool geometry by simulating the hobbing process. The gear pair contact line was numerically defined direct from the gear surface geometry. The constructed model used 3D finite elements for the calculation of tooth deflection including tooth bending, shearing and tooth foundation flexibility. The model combined contact analysis and structural analysis to avoid large meshes. The flexibility of tooth foundation was found to have an essential role in contact load sharing between the meshing teeth, whereas contact flexibility plays only a minor role. This indicates that reasonable distribution of tooth contact force along the line of action may be generated by using flexible teeth and flexible tooth foundation, but allowing rigid contact. The FEM-based contact model gave a reasonable approximation of contact parameters when the mesh size was fine.

Chen et al. (2002) performed finite element stress analysis to investigate the contact stress and the bending stress of a modified helical gear set comprising an involute pinion and a modified helical gear. The FEA tooth models including the working surfaces and the fillets of the pinion and the gear were developed. Commercial FEA software ABAQUS was utilized to evaluate the stress distribution on the tooth surfaces. The analysis results revealed that, the proposed helical gear set exhibited localized bearing contacts due to double crowning on the gear's tooth surfaces. The contact stress calculated by FEA were close to the Hertzian contact stress obtained from the Hertzian stress formulae and curvature analysis. Increasing $R_l(G)$(radius of the circular-arc cutting edges) resulted in an increase in the contact area and a reduction in contact stress, due to a smaller lengthwise crowning effect on the gear's tooth surfaces. Although a larger $R_l(G)$ caused a smaller profile crowning effect, the reduction of contact stress was less significant than the influence of $R_l(G)$. The tensile and compressive bending stresses along the pinion's fillets under diIerent contact positions were investigated. The maximum fillet stress was found near the middle section of the tooth fank.

Li (2008) examined the vibration conduct of the three-dimensional, thin-walled gears from experimental tests and theoretical breaks down. It was discovered that vibration conduct of the thin-walled apparatus was not quite the same as the thick-walled gears in that vibration of thick-walled gears was tooth-bending vibration with single recurrence while vibration of the thin-walled rigging was structural vibration of the edge and web with multi-frequencies. Resonance frequencies of the thin-walled gears were explored in a force coursing structure

test apparatus at the rate extend 500–3000 rpm. It was observed that when the divider thickness was thin, vibration of the thin walled rigging was the second, the third, the fourth request edge bending vibrations and the second, the third and the fourth request web bending vibrations. At the point when the divider thickness was expanded, the second, the third and the fourth request web bending vibrations vanish and just the second, the third and the fourth request edge bending vibrations are remained. "Strain Phase Method" was displayed to measure resonance mode states of the thin-walled goad gear when the rigging runs in a totally resonance state. The measured mode states of the thin walled apparatus were concurrence with the ascertained ones. Element burden components and top paces of the thin-rimmed rigging were measured at the velocity go 500–3000 rpm when there were misalignment slip and no misalignment blunder for the gears. It was discovered that the fourth request edge bending vibration was one of essential mode shapes for structural vibration of the thin-walled rigging. It was additionally discovered that top velocities of the thin-rimmed rigging were influenced by gathering lapses. 20-hub isoperimetric strong component and FEM were utilized to perform characteristic vibration analysis of the thin walled apparatus structures. Regular frequencies and mode states of the thin-walled gears computed by the FEM were well concurrence with the measured ones. Impacts of apparatus module and structural measurement parameters of the thin-walled rigging on characteristic frequencies of the apparatus were examined by performing FEM computations. It was observed that edge and web thickness have more noteworthy impact on the regular frequencies of the thin-walled rigging than different parameters. With the augmentations of web and edge thickness, all the characteristic frequencies of the thin-walled apparatus get to be ever more elevated. Gear module, web position and apparatus face width likewise influence structural frequencies of the thin walled rigging, however the impacts of these parameters were not all that more noteworthy than the edge and web thick.

Lin et al. (2007) proposed a finite element method for 3D dynamic contact/impact problems. This method was based on the derivation of the effective flexibility matrix equation, which was condensed from the global motion equations to the contact region of 3D dynamic contact/impact problems. A computer program was developed, which includes an automatic mesh generation, simulation of static and dynamic contact analysis particularly for the contact/impact problems of gear drives. The meshing performance and impact characteristics for both the spur and the helical gear drives were simulated under specifically defined gear operation conditions. The mesh stiffness results during the operation process obtained from this agree well with the results calculated from the conventional method. When the case of

initial speed impact was considered, the contact time was independent from the initial speed but the total contact force was directly proportional to the initial speed. The more the tooth pairs were engaged, the less variance of the impact forces was. The results also quantify the differences of the total contact forces between the spur and helical gear drives. The approach impact time was mainly prescribed by the geometric parameters of the gear drive and the total approach contact force was directly proportional to the initial speed and the sudden load. The tooth engagement was delayed because of the tooth backlash. For the sudden load impact problem, the delay time was proportional to the value of the backlash. The total contact force increases significantly with the increase of the tooth backlash but the contact time reduces slightly.

Shinde et al. (2012) proposed a parametric model which was capable of creating spur gears with different modules and number of teeth by modifying the parameters and regenerating the model. Sets of gears having the same module and pressure angle could be created and assembled together. It was possible to carry out finite element analysis such as root bending stress and contact stresses between gear teeth pair and effect of root fillet radius on the root stresses. The model was applied onto commercial FEA software ANSYS. Simulation results were compared and confirmed by the theoretical calculation data. According to these results, a conclusion was drawn; that the numerically obtained values of stress distributions were in good agreement with the theoretical results. This study provided a sound foundation for future studies on contact stresses.

Cavdar et al. (2005) developed a tooth model of involute spur gears with asymmetric tooth. A computer program, estimating the variation of maximum bending stress and contact ratio depending on tooth number and pressure angle of the drive side, had been developed for asymmetric drives. The bending stress analyses had been performed with the aid of FEM for asymmetric and symmetric tooth. The stress results obtained by FEM analyses and estimated by the developed program have been compared. It had been proved that asymmetric teeth had better performance than both symmetric teeth with common pressure angles 20 deg and 25 deg and symmetric teeth with high pressure angle for bending stress minimization. It had been confirmed that, as the pressure angle on the drive side increases, the bending stress decreases and the bending load capacity increases. It had been seen that, while the value of maximum bending stress was changing, the location of maximum bending stress remains the same in finite element analysis.

Kapelevich et al. (2003) presented the engineering method for bending stress balance and minimization. Optimization of the fillet profile allows reducing the maximum bending stress

in the gear tooth root area by 10–30%. It works equally well for both symmetric and asymmetric gear tooth profiles.

Mallesh et al. (2009) proposed as the number of teeth and module increases the bending stresses decreases, while the other parameters were unchanged. This was due to the fact that with increase of module, the pitch diameters of the gear tooth increases causing the tooth to become bulkier and stronger. Again with the increase of module, the fillet radius of the tooth increases which would cause less impact in the root region (critical section) of the gear tooth. The increase of module means the increase of the tooth width from top to bottom, as a result the stress was observed to be less in the wider tooth for the same loading. The bending stresses decreased with increases in the number of teeth and pressure angle on drive side, with the application of the same load for all gear teeth and one with more teeth it was observed that as the pressure angle on the drive side increases bending stress decreases.

Rathore et al. (2014) proposed the process of optimization of spur gear bending stress and related fatigue life. It was done with the help of some stress relief features like holes. The methods of choosing the size and location of the hole was also proposed. This led to unique results where the bending stress had been reduced to 21% approximately. The bending stress was calculated with FEA analysis and comparison of FEA stress was done with the stress calculated from AGMA standard, both the results was in good agreement.

3.1 Gaps in literature

It is known that farming equipments are often overdesigned. A review of literature provided useful information regarding gear tooth analysis conducted on different gears. But a detailed analysis on rotavator gears has not been reported. To fulfill this gap, stress and mode shape analysis is performed on gears of a rotavator manufactured in India.

3.2 Problem formulation

Stress analysis and modal analysis of spur gears employed in a rotavator.

3.3 Objectives of the study

1. Stress analysis and modal analysis of gears using finite element analysis software
2. Validation of results of stresses obtained using FE model.
3. Design modifications in gears with an objective to reduce stresses and weight of gears.

4.1 Gear geometry

First and the foremost step is to prepare CAD model of gears accurately. The most complicated step in CAD modeling of spur gear is to create the involute profile of its teeth. There are many ways of creating involute profile of a spur gear. In this work the spur gear model was created in CREO by PTC. CREO is a suite of programs, which are basically used in designing and manufacturing wide range of products.

Solid modeling means that the computer model contains all the information that a real solid object would have. It has volume and so, if one provides a value for density of its material, it has mass and inertia. Solid model differs from surface model on the pact that if a hole or a cut is made in a solid model, a new surface is automatically created and the model knows which side of surface is solid material. One of the best features of solid modeling is that it is impossible to create a computer model that is ambiguous or physically non-realizable. The gears dimensions are given in table 4.1.

Table 4.1 Geometrical parameters of Spur gears

Upper Gear		Idler Gear		Lower Gear	
Module	7	Module	7	Module	7
No of teeth	25	No of teeth	35	No of teeth	26
Pitch Circle Dia	175	Pitch Circle Dia	245	Pitch Circle Dia	182
Add. circle Dia	189	Add. circle Dia	260	Add. circle Dia	196
Ded. Circle Dia	157.5	Ded. Circle Dia	228	Ded. Circle Dia	164.5
Pressure Angle	20	Pressure Angle	20	Pressure Angle	20

4.2 General involute profile

The involute of a circle is the spiraling curve traced by the end of an imaginary taut string unwinding itself from that stationary circle called the base circle. The CAD models of gears are given in fig. 4.2, 4.3 and 4.4, and assembly views are given in 4.5 and 4.6.

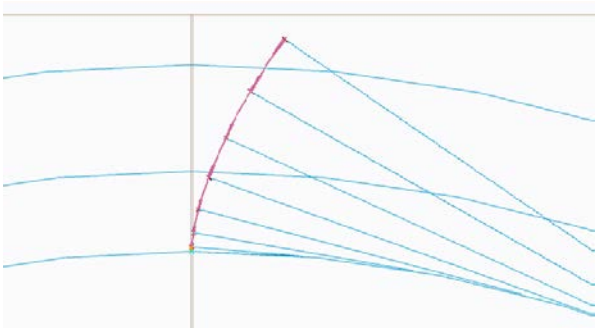

Fig. 4.1 Involute profile

4.3 Finite element models: Gears & Assembly

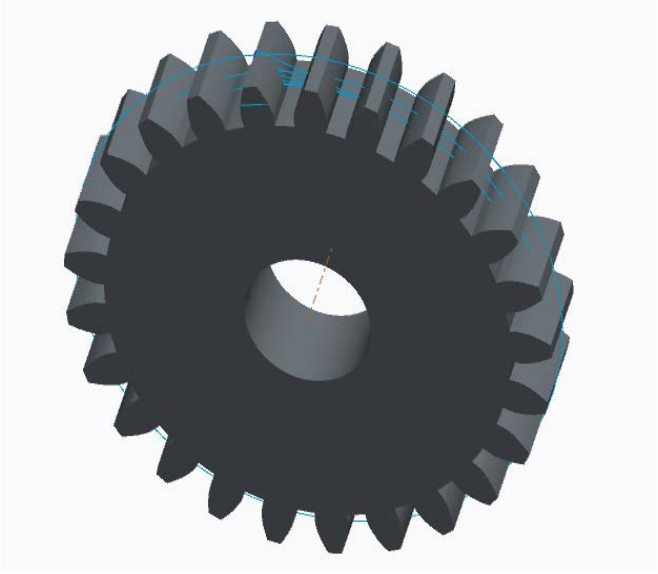

Fig. 4.2 CAD model of upper gear

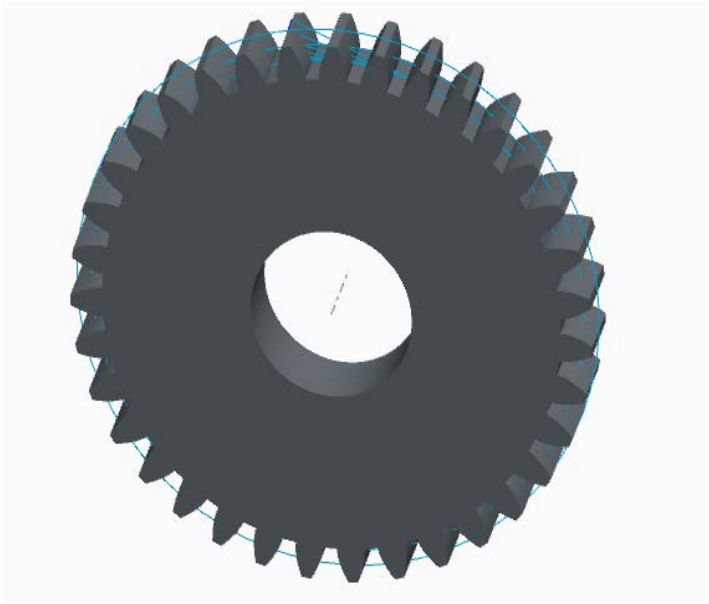

Fig. 4.3 CAD model of idler gear

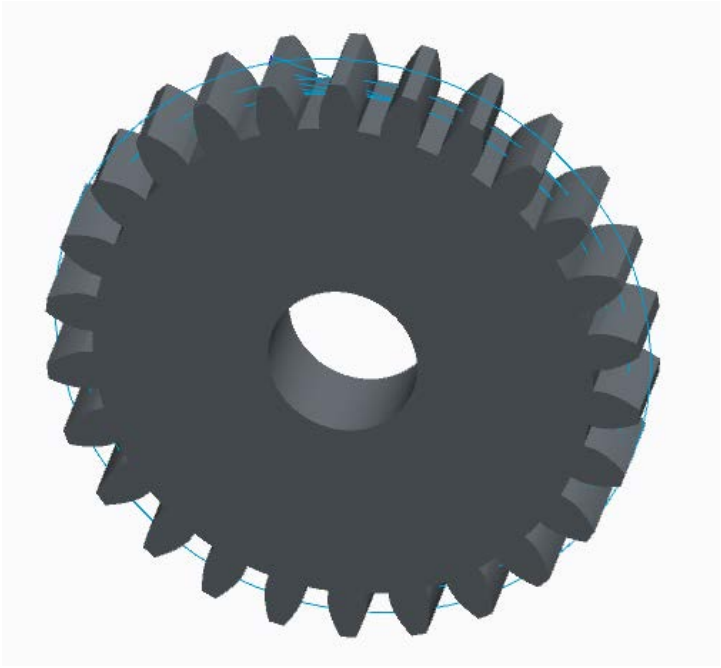

Fig. 4.4 CAD model of lower gear

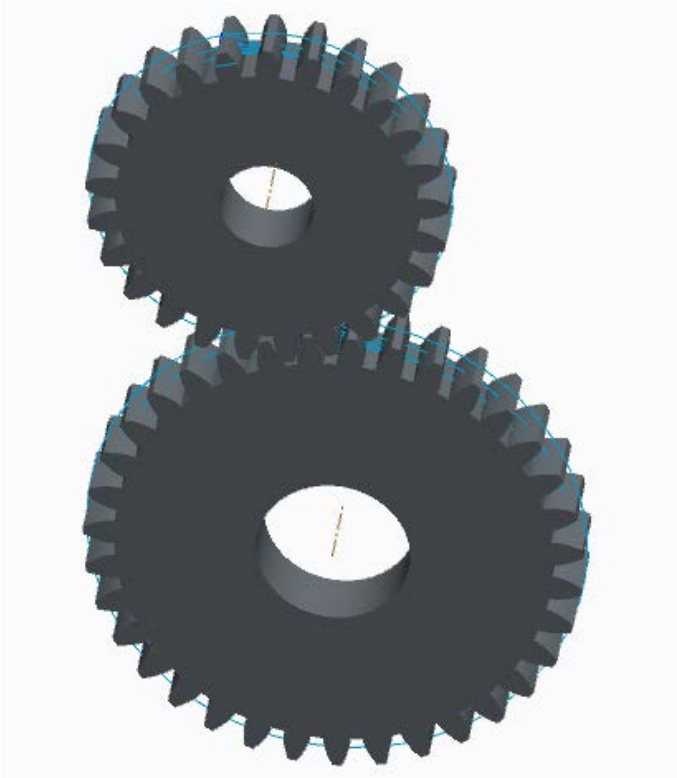

Fig. 4.5 Assembly view of upper and idler gear

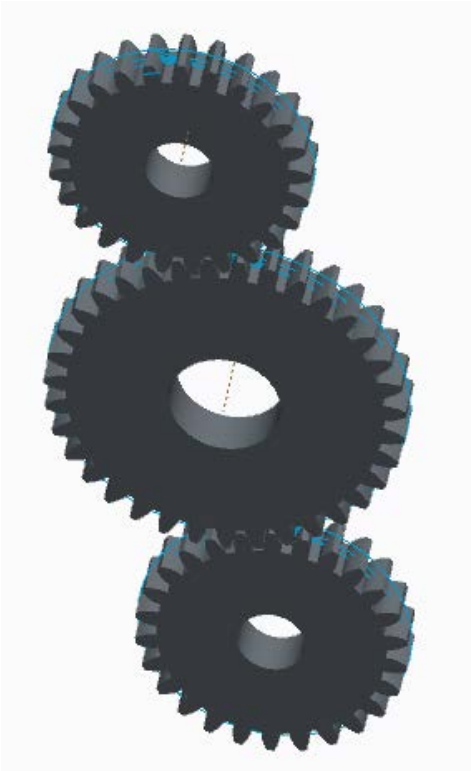

Fig. 4.6 Assembly view of gear train

4.4 Finite element analysis of gears.

4.4.1 Procedure

Different models of spur gear were created, using the assembly option in CREO. Assembly was created corresponding to the models. The assembly, which was created in CREO, was imported in ANSYS Workbench 14 for further analysis. The other way of importing the assembly is by importing the IGES or STEP file of the assembly. The material properties assigned to model are given in table 4.2.

Table 4.2 Material properties [22]

Material	EN353
Modulus of elasticity	221 GPa
Poission ratio	0.264
Yield strength	320 MPa

The boundary conditions imposed after the assembly is imported in ANSYS Workbench 14. In this work it is assumed that the one gear is fixed and the other gear is given 965539.9881 N-mm torque along its axis

4.4.2 Three dimensional stress analysis

4.4.2.1 Bending stress analysis

ANSYS has many type of analysis, so it is necessary to select the correct type of analysis from the menu bar. As the imported geometry is 3-Dimensional, select 3-D and Static Structural Analysis from menu and connect the geometry to the analysis tab. Then the next step is to enter the Young's modulus and poisson's ratio of the material. This can be done by selecting the engineering data from the analysis tab and inserting the corresponding values.

Defining contact region

Once the geometry is attached with static structural analysis tab, next thing is to define the contact between the two involute teeth. ANSYS has an inbuilt option, which automatically reads the attached geometry for any predefined contacts or other boundary definitions. The contact between the two teeth is assumed to "No-separation" (fig. 4.7). It is a rigid contact or also known as linear contact.

Scope	
Scoping Method	Geometry Selection
Contact	1 Face
Target	1 Face
Contact Bodies	gear_25_upper.prt
Target Bodies	gear_35_middle.prt
Definition	
Type	No Separation
Scope Mode	Manual
Behavior	Program Controlled
Suppressed	No

Fig. 4.7 Defining contact for bending stress analysis

Mesh generation

Discretization is the method of converting continuous models to discrete parts. The goal is to select and locate finite element nodes and element types so that the associated analysis is sufficiently accurate. Element Aspect ratio must be near unity to obtain accurate results. For

the current analysis average aspect ratio is obtained as 1.84 by setting the mesh relevance to fine and smoothing to medium and span angle center to coarse. Tetrahedron elements are used since stress is present all alone the thickness of the part. A patch independent algorithm is used since a finer mesh is required around edges and corner. For rest of the body a normal mesh is sufficient and in advanced meshing features the proximity and curvature feature needs to turned on since the curvature size function examines the curvature on the faces and edges and computes the element sizes so that the element size doesn't exceed the maximum size of curvature angle which are either defined by the user or taken automatically.

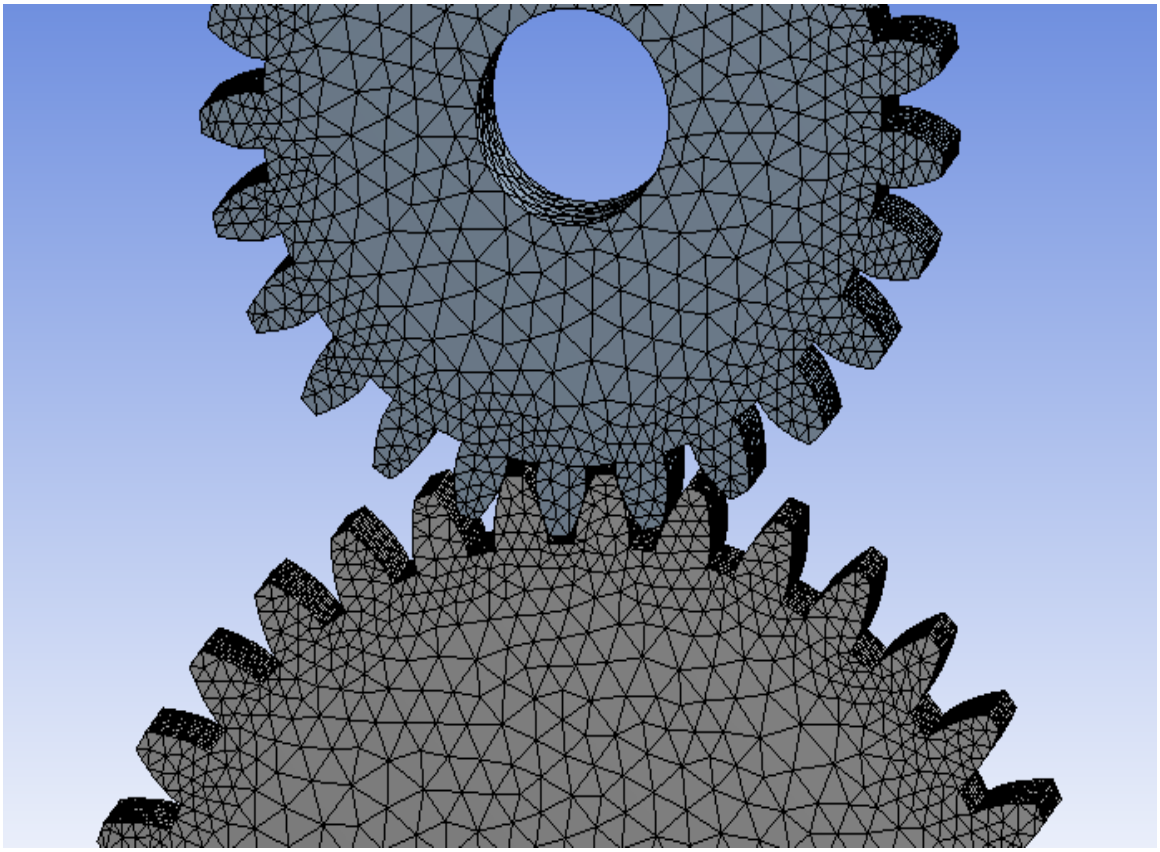

Fig. 4.8 Meshed FE model

Supports and loads

The lower gear is given a fixed support and the top gear is given cylindrical support. The top gear is also given a toque or a moment in clockwise direction. The fig. 4.9 shows how the supports and loads were applied to the gear model.

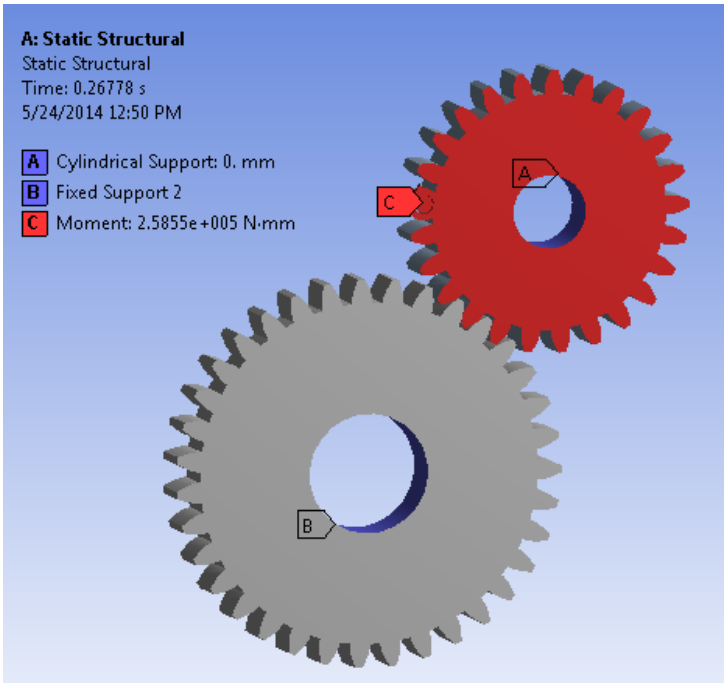

Fig. 4.9 Applied boundary conditions

Root bending stress of spur gear

Using ANSYS, three dimensional root bending stresses are obtained. The maximum equivalent bending stress is 117.22 MPa (fig. 4.10) located at root of tooth.

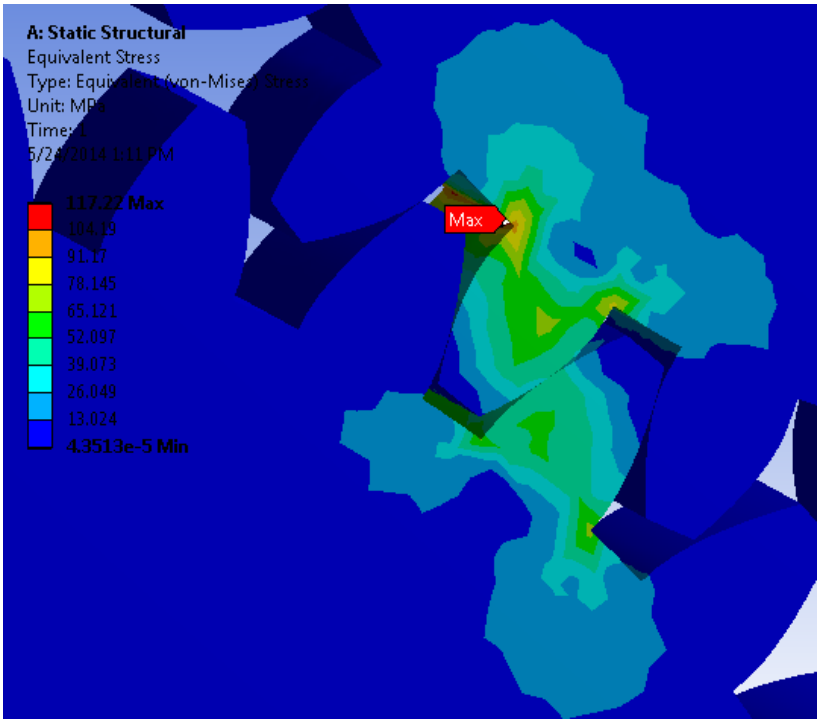

Fig. 4.10 Three dimensional equivalent von-Mises stress (bending) in upper and idler gear assembly

4.4.2.2 Contact stress analysis

As already mentioned high contact stresses results in pitting failure of the gear tooth, it is necessary to keep contact stresses under limit. In this work von-Mises Contact stresses are obtained at the contact region.

Defining contact region for contact stress

The contact between the two teeth is assumed to "Frictional contact" also known as nonlinear contact (fig. 4.11). The coefficient of contact of gear tooth surface is situated to 0.4. In this setting, Augmented Lagrange is chosen as the solver for the contact non-linearity problem. The normal force exerted by the target on the contact face is calculated as

$$F_{normal} = k_{normal} x_{penetration} \tag{4.1}$$

Where

k_{normal} is contact stiffness.

Augmented Lagrange formulation has an extra term λ to the equation. This makes the penalty less sensitive to penetration. This method usually leads to better conditioning and is less sensitive to the magnitude of the contact stiffness coefficient.

Scope	
Scoping Method	Geometry Selection
Contact	1 Face
Target	1 Face
Contact Bodies	gear_25_upper.prt
Target Bodies	gear_35_middle.prt
Definition	
Type	Frictional
Friction Coefficient	0.4
Scope Mode	Manual
Behavior	Program Controlled
Suppressed	No
Advanced	
Formulation	Augmented Lagrange
Detection Method	Program Controlled
Interface Treatment	Adjust to Touch
Normal Stiffness	Program Controlled

Fig. 4.11 Defining contact for contact stress analysis.

Meshing, supports and load

Mesh is generated with the same procedure as generated in bending stress. The finite element model used in bending analysis is used here.

Contact stress result

Using ANSYS, three dimensional contact stresses are obtained. The maximum equivalent contact stress obtained is 152.55 MPa (fig. 4.12).

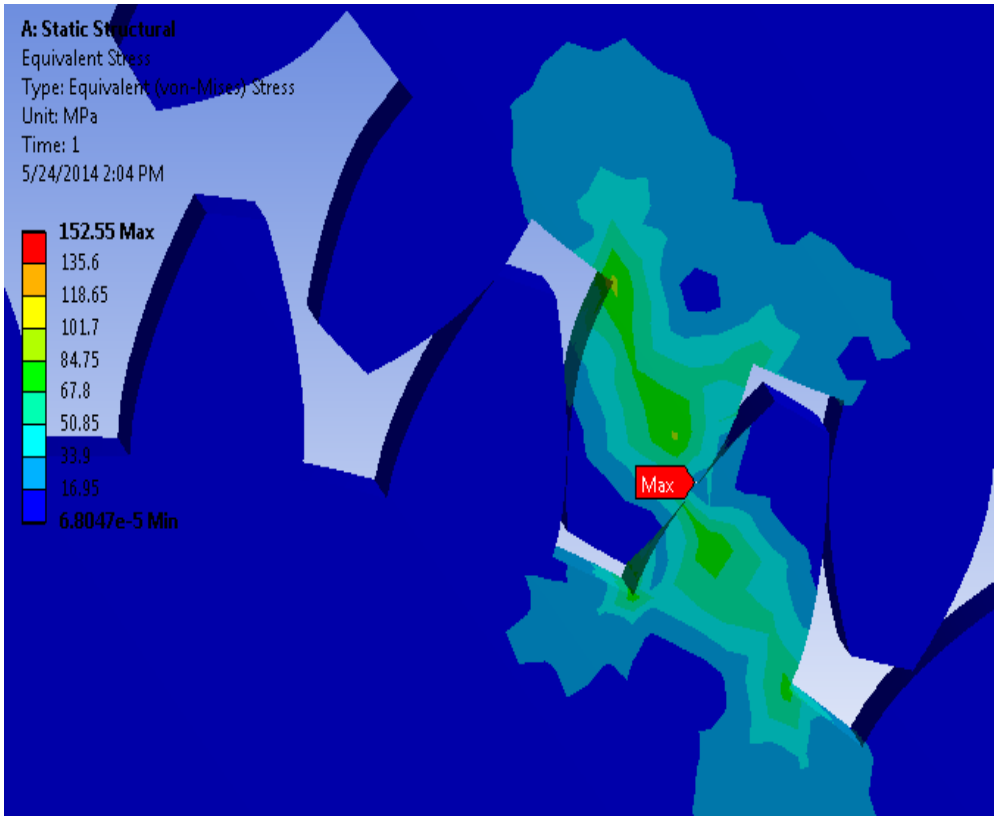

Fig. 4.12 Three dimensional equivalent von-Mises stress (contact) in upper and idler gear assembly.

4.5 Validation of bending and contact stress results obtained from FEA.

The results obtained from FEA analysis are verified by comparing them with the standard theoretical procedures. FEA bending stresses are validated by comparing them with standard Lewis bending stress equations and FEA contact stresses are compared with the Hertz contact stresses.

Bending stress validation

As mentioned in the above section standard bending stress is compared with the Lewis bending stress equation. This value can be calculated from equation 1.1.

Gear specifications

Number of Teeth N: 25

Diametrical Pitch P_d: .1428

Pressure Angle Ø: 20°

Face Width b: 35 mm

Lewis Form Factor Y: 0.37

Now from the above gear specifications, Lewis bending stress from equation 1.1 is obtained as

$$\sigma_{lewis} = \frac{10484.95 \times .1428}{.37 \times 35}$$

$$\sigma_{lewis} = 115.61\ MPa$$

Bending stress obtained from FE Analysis is given by

$$\sigma_{FEA} = 117.52\ MPa$$

Validation of contact stress

As mentioned above contact stress obtained from FEA is verified by comparing them to Hertz Contact stress. The following are the specifications and other factors used for calculation of the hertz contact stress

Modulus of Elasticity E: 221000 MPa

Poisson's Ratio μ: 0.246

Load W: 335.51 N/mm

Pitch circle radius of pinion rb_1: 87.5 mm

Pitch circle radius of gear rb_2: 122.5 mm

From above parameters the contact stress is given by the equation 1.9

$$\sigma_{Hertz} = \sqrt{\frac{335.51(1 + \frac{87.5}{122.5})}{[87.5 \times 35 \times 3.14\{\frac{1 - .264^2}{221000}\} \times 2] \times sin20^{\circ}}}$$

$$\sigma_{Hertz} = 144.35\ MPa$$

Bending stress obtained from FE Analysis is given by

$$\sigma_{FEA} = 152.55\ MPa$$

Table 4.3 Validation of FEA results

Stress	Theoretical Values	FE Results	Percentage Error
Bending Stress	115.61 MPa	117.52 MPa	1.60%
Contact Stress	144.35 MPa	152.55 MPa	5.37%

Thus the results obtained by FEA are in good conformance with the analytical results.

4.6 Modal analysis of spur gear train

Modal analysis is used to determine the vibration characteristics (natural frequencies and mode shapes) of a structure or a machine component while it is being designed. It can also serve as a starting point for another, more detailed, dynamic analysis, such as a transient dynamic analysis, a harmonic response analysis, or a spectrum analysis.

ANSYS Workbench is used to apply the motion constraints and contact conditions. There are two separate conditions being analyzed in conducting modal analysis of the gear trains. The initial six natural frequencies and their mode shapes are examined on the gear train without pre-stress state including constraints only and pre-stress state which is comprehensive of loads and constraints.

4.6.1 Modal analysis of gear train in free stress state

The first six mode shapes and their natural frequencies of the gear train involving constraints only considering single pair tooth contact and double pair tooth contact.

4.6.1.1 Modal analysis of gear train in free stress state and single pair tooth contact

Defining contact

No-separation contact is applied. as shown in fig 4.13

Scope	
Scoping Method	Geometry Selection
Definition	
Type	No Separation
Scope Mode	Manual
Behavior	Program Controlled
Suppressed	No
Advanced	
Formulation	Program Controlled
Detection Method	Program Controlled
Normal Stiffness	Program Controlled
Update Stiffness	Program Controlled
Pinball Region	Program Controlled

Fig. 4.13 Defining contacts of the gear train with one idler gear

Meshing of the spur gear train.

After imported the assembly of gear train in Modal analysis of Ansys workbench, each gear model is so meshed with Tetrahedron elements to obtain an aspect ratio of 1.98.

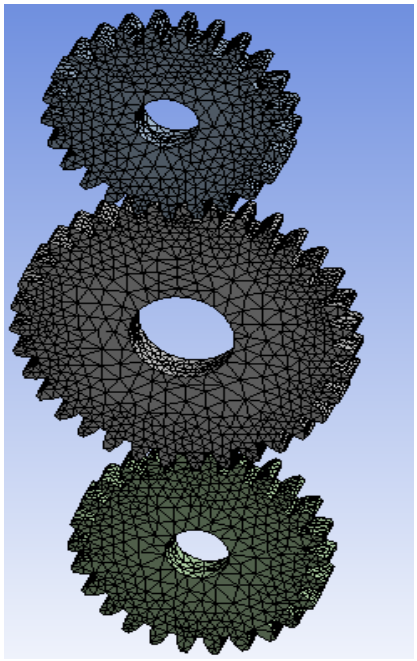

Fig. 4.14 Meshed model of the gear train with one idler gear

Supports applied

In the free stress state, cylindrical supports are assumed as the bearing supports for the gears, which permits rotational movement along the pole hub but restricts axial movement and radial movement as shown in fig 4.15.

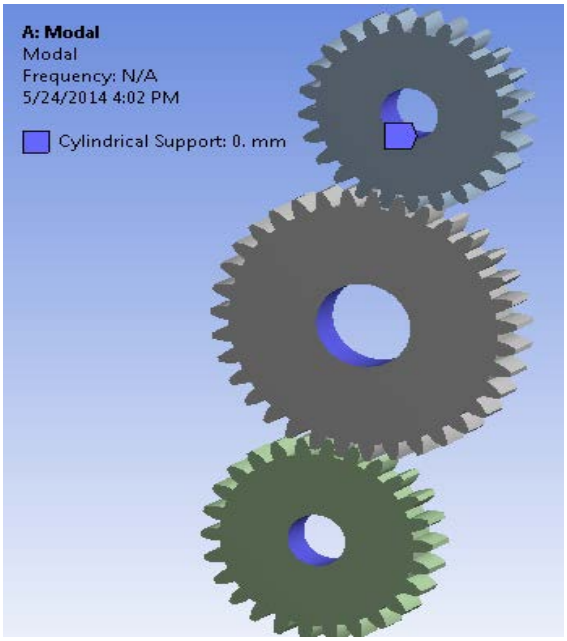

Fig. 4.15 Cylindrical support applied to three different gears.

Mode shapes of the gear train

Mode shapes of the gear train in free-tress state and single pair tooth contact as shown in fig 4.16.

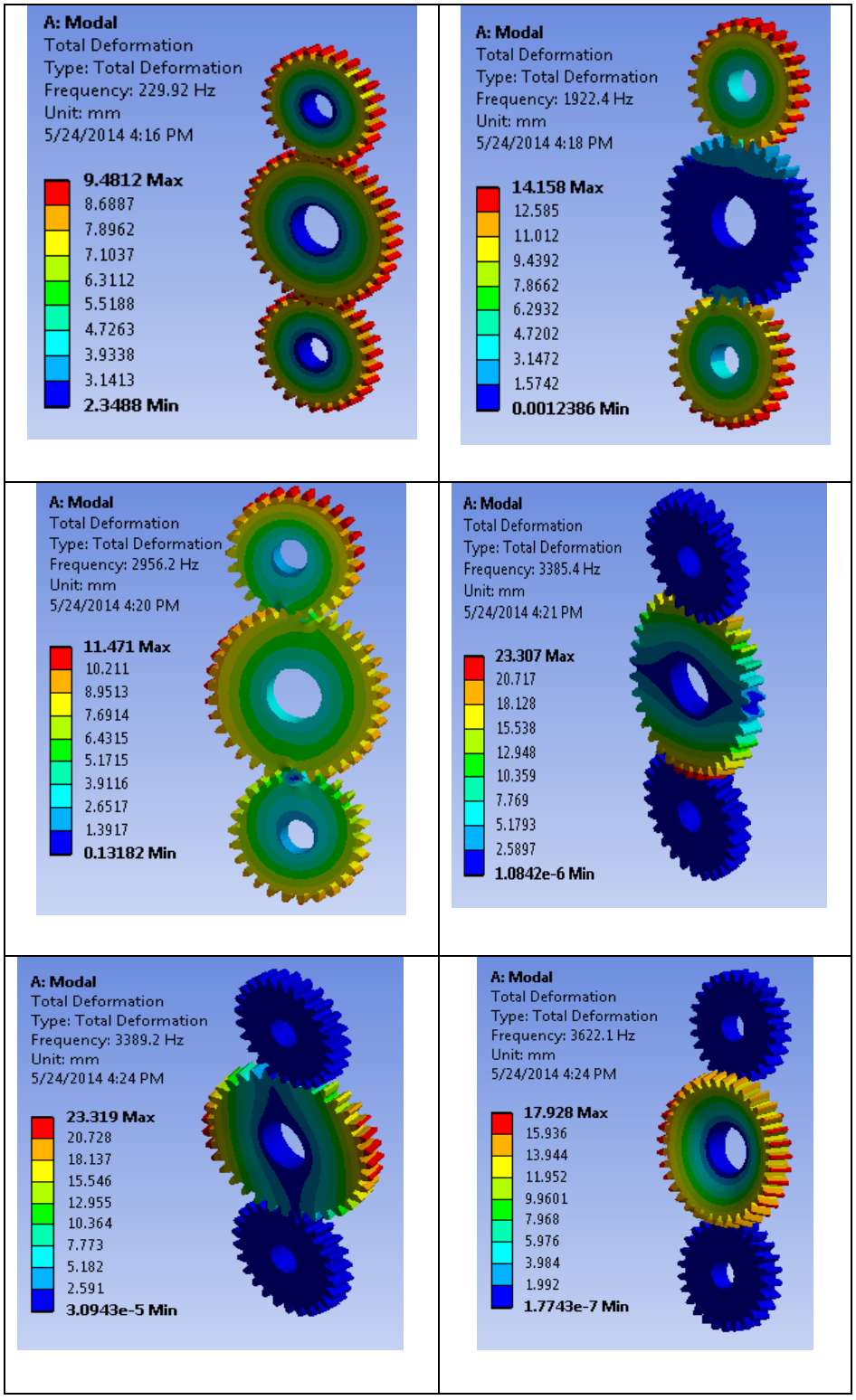

Fig. 4.16 First six mode shapes of the gear train in free stress state and single pair tooth contact.

Natural frequencies

Fig. 4.17 shows first six natural frequencies of the gear train in free stress state and single pair tooth contact.

Mode	Frequency [Hz]
1.	229.92
2.	1922.4
3.	2956.2
4.	3385.4
5.	3389.2
6.	3622.1

Fig. 4.17 First six natural frequencies of gear train in free stress state and single pair tooth contact

4.6.1.2 Modal analysis of gear train in free stress state and double pair tooth contact

Mode shapes of the gear train

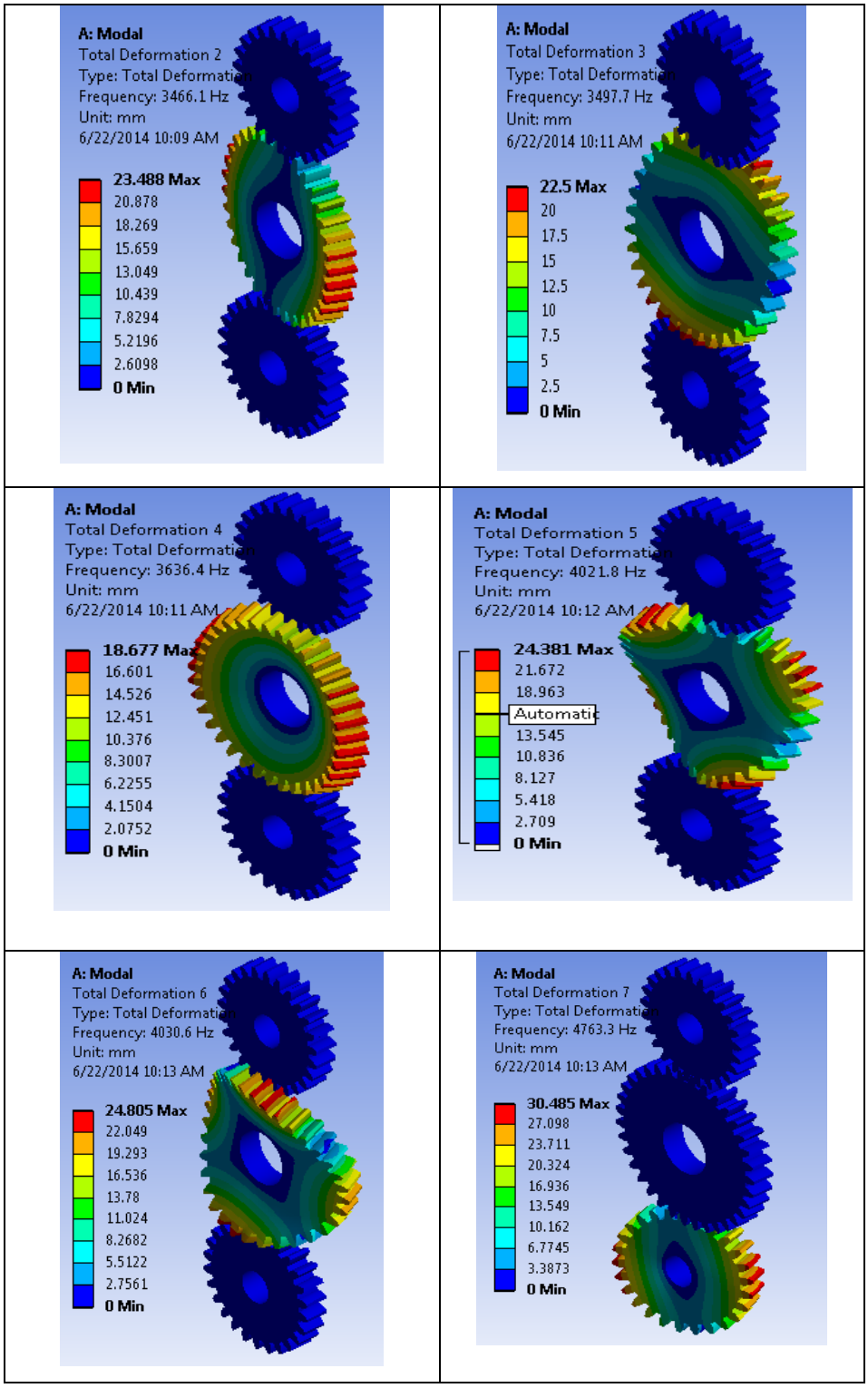

Fig. 4.18 First six mode shapes of the gear train in free stress state and double pair tooth contact.

Natural frequencies

Fig. 4.19 shows first six natural frequencies of the gear train in free stress state and double pair tooth contact.

	Mode	Frequency [Hz]
1	1.	3466.1
2	2.	3497.7
3	3.	3636.4
4	4.	4021.8
5	5.	4030.6
6	6.	4763.3

Fig. 4.19 First six natural frequencies of gear train in free stress state and double pair tooth contact

4.6.2 Modal analysis of gear train in pre-stress state

In it first six mode shapes of the gear train with one idler gear and their natural frequencies are obtained with pre-stress state inclusive of constrains and loads, during single pair tooth contact and double pair tooth contact.

.

4.6.2.1 Modal analysis of gear train in pre-stress state and single pair tooth contact

Contacts and meshing

Contacts and meshing are same as that of free-stress state.

Supports and loads

In the pre-stressed state of the gear train, the cylindrical supports are situated the same as the one in the free stress state. Also a gravitational load because of the segment's weight is applied and a torque load of 965539.9881 N-mm is applied at the input gear shaft. The cylindrical surface of the output gear shaft is completely constrained to create static loading condition. In pre-stress state, the stress because of moment and gravity was calculated first before modal analysis is applied.

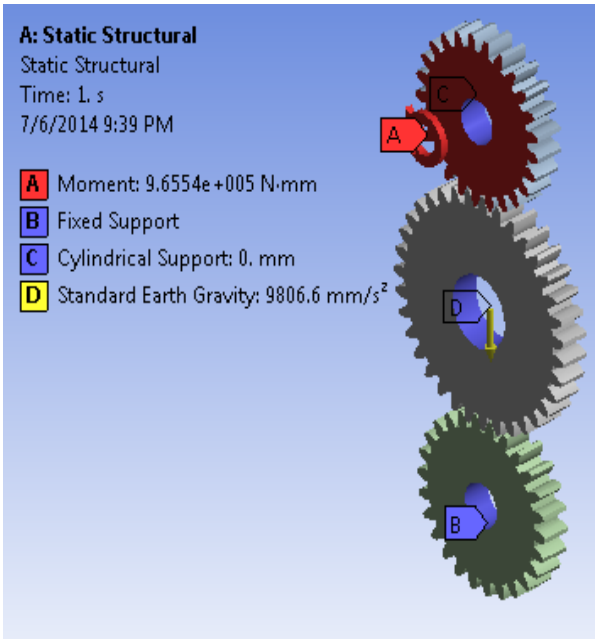

Fig. 4.20 Supports and load applied to the gear train

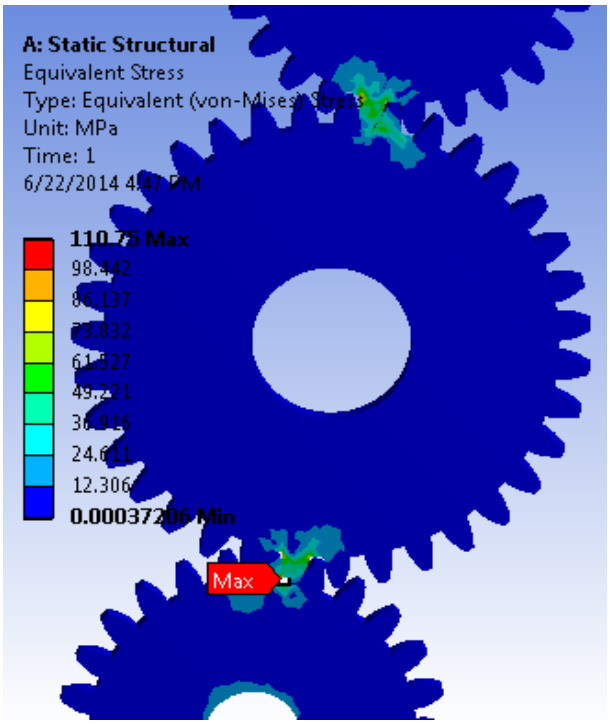

Fig. 4.21 Equivalent stress (bending) in the gear train with one idler gear and single pair tooth contact

Table 4.4 Maximum equivalent (bending) stress value in gear train with one idler gear and single pair tooth contact

Maximum equivalent Stress	110.75 MPa

Mode shapes of the gear train

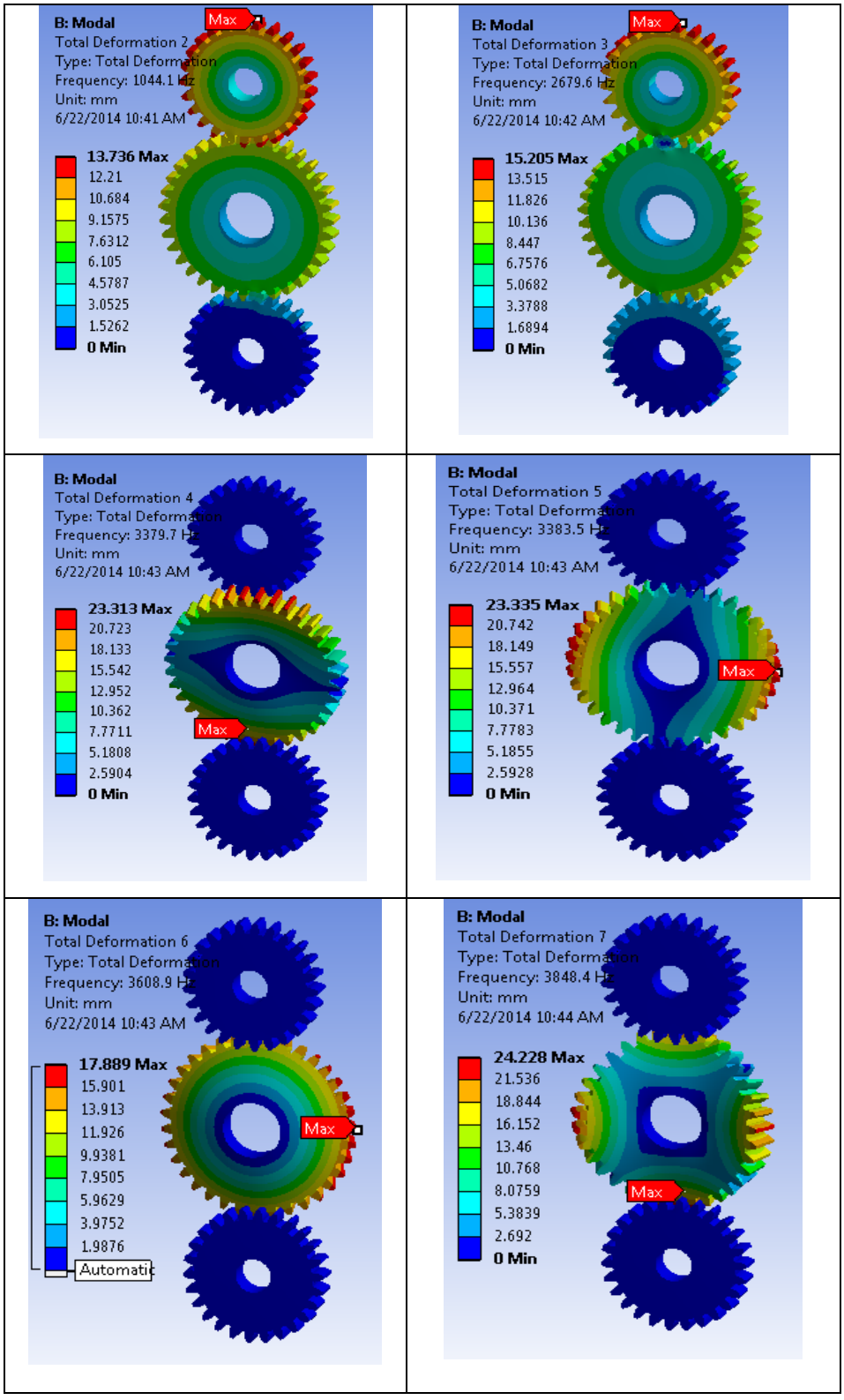

Fig. 4.22 First six mode shapes of the gear train in pre-stress state and single pair tooth contact.

Natural frequencies

Fig. 4.23 shows first six natural frequencies of the gear train in pre stress state and single pair tooth contact.

	Mode	Frequency [Hz]
1	1.	1044.1
2	2.	2679.6
3	3.	3379.7
4	4.	3383.5
5	5.	3608.9
6	6.	3848.4

Fig. 4.23 First six natural frequencies of gear train in pre-stress state and single pair tooth contact

4.6.2.2 Modal analysis of gear train in pre-stress state and double pair tooth contact

Equivalent stress during double pair tooth contact.

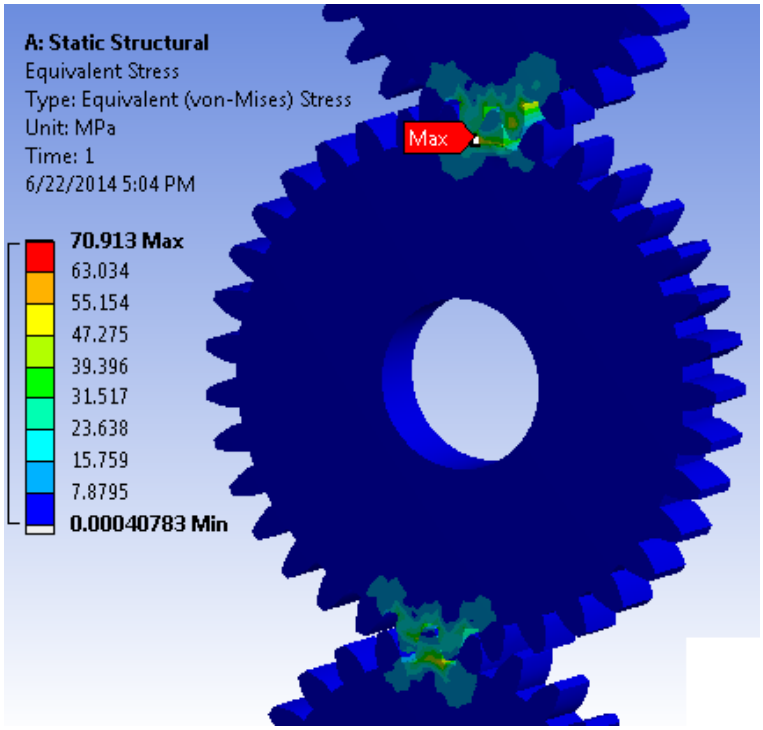

Fig. 4.24 Equivalent stress (bending) in the gear train with one idler gear and double pair tooth contact

Table 4.5 Maximum equivalent (bending) stress value in gear train with one idler gear and double pair tooth contact

Maximum equivalent Stress	70.913 MPa

Mode shapes of the gear train

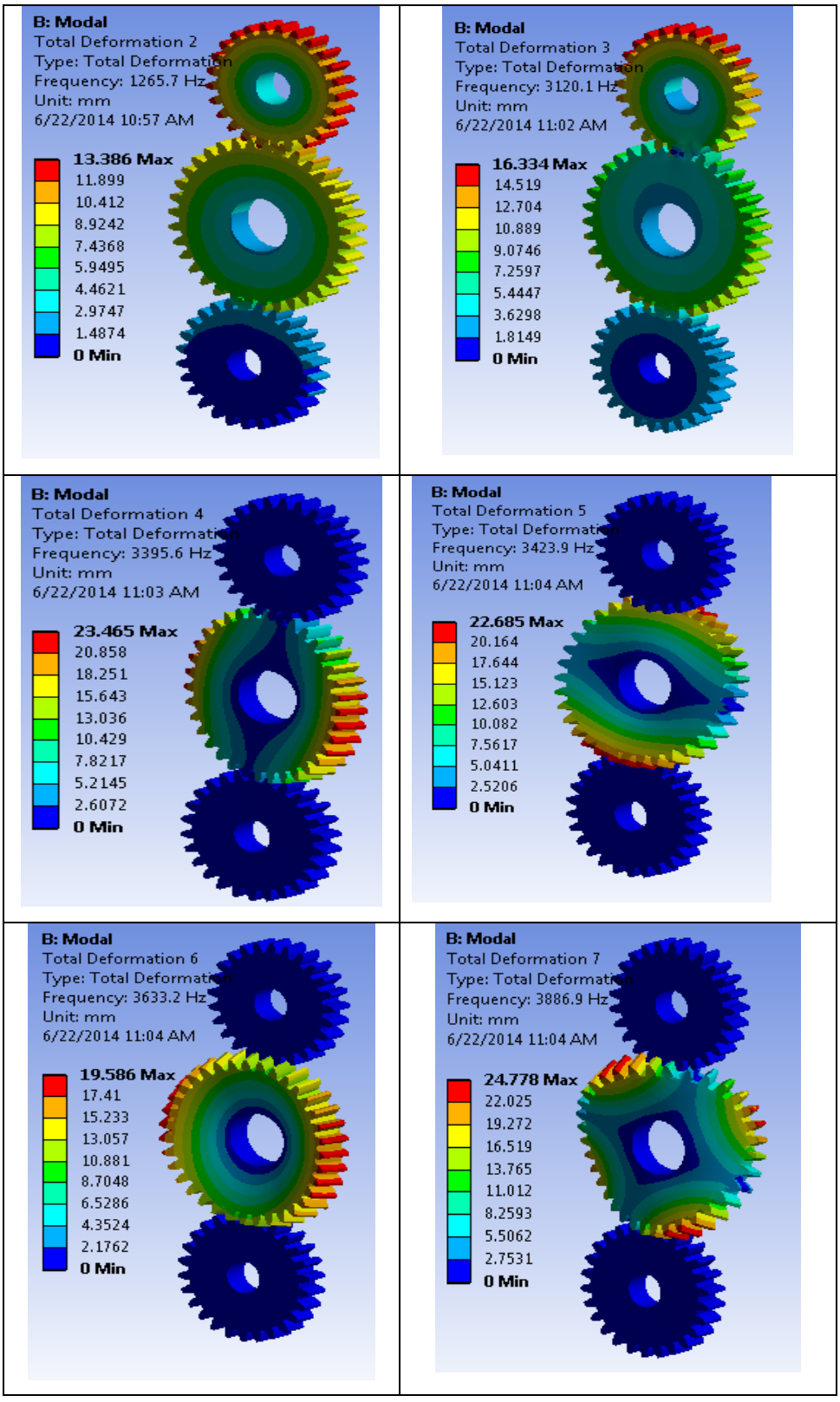

Fig. 4.25 First six mode shapes of the gear train in pre-stress state and double pair tooth contact.

Natural frequencies

Fig. 4.26 shows first six natural frequencies of the gear train in pre stress state and double pair tooth contact.

	Mode	Frequency [Hz]
1	1.	1265.7
2	2.	3120.1
3	3.	3395.6
4	4.	3423.9
5	5.	3633.2
6	6.	3886.9

Fig. 4.26 First six natural frequencies of gear train in pre-stress state and double pair tooth contact

Modal analysis on spur gear train is studied using FEA, and mode shapes and natural frequencies are calculated while the gear train subjected to single pair tooth contact and double pair tooth contact. Lowest natural frequency is compared with operating frequency range of gear train of a rotavator (obtained from manufacturer), and found that operating frequency range is 3.75 Hz to 4.5 Hz which is much low as compare to lowest natural frequency i.e. 229 HZ.

5.1 Methods of reducing stress concentration on gear tooth

Gear tooth failure due to higher stress concentration is a general incident observed. Yet a minor drop in stress concentration results in enhancement of the life of a spur gear. A number of methods up till now has been adopted to enhance the life of a spur gear, the methods are use of better material, surface hardening and carburization etc. The majority of these techniques do not provide assurance for the interchangeability of the existing gear design. This work shows the potential by means of stress concentration methods by inserting the stress relieving features [20]. In this work circular pocket is cut from the both sides of gear web and after that bending, contact stress and modal analysis are performed.

5.2 Effect of reducing web thickness

An analysis on weakest gear is performed to determine effect of varying diameter of pocket cut in the web. The variation of bending stresses and contact stresses are shown in fig. 5.1 and 5.2 respectively. The bending stress and contact stress distribution calculated with 145 mm pocket diameter are shown in fig. 5.3 and 5.4. (Bending stress value is 103.1 MPa, Contact stress value is 139.21 MPa)

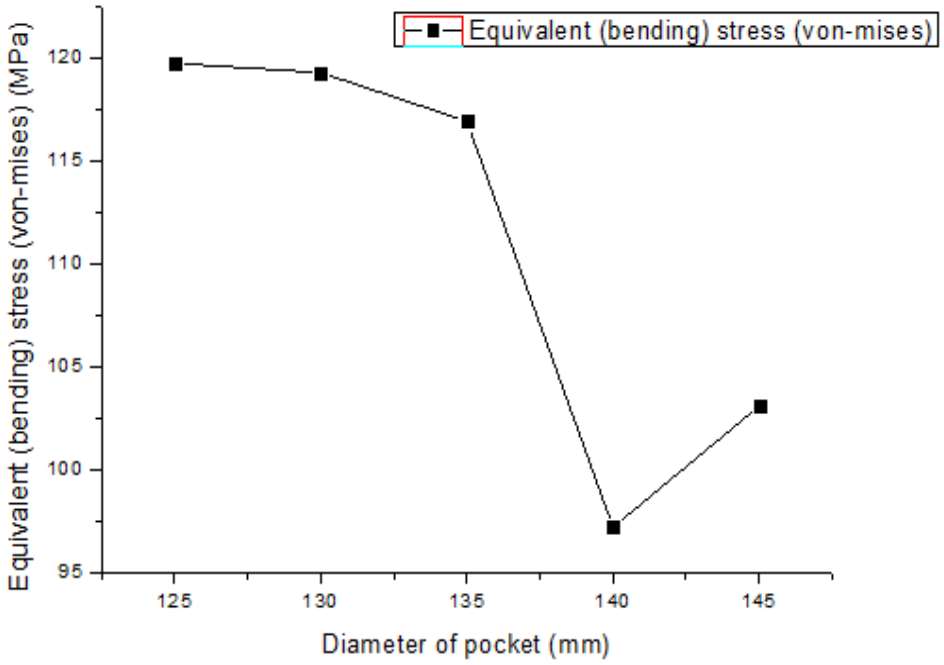

Fig. 5.1 Equivalent bending stress at different diameters of pocket

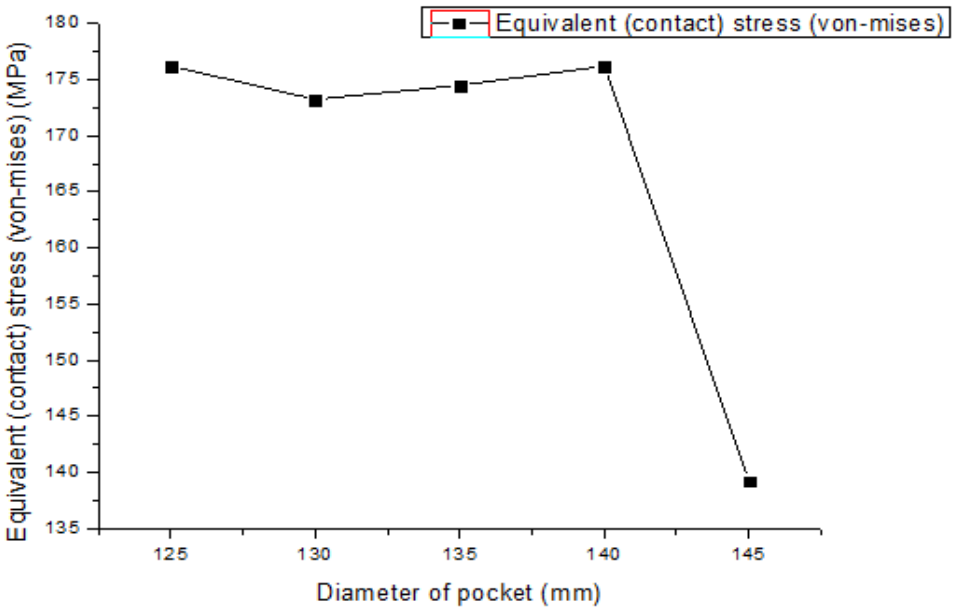

Fig. 5.2 Equivalent contact stress at different diameters of pocket

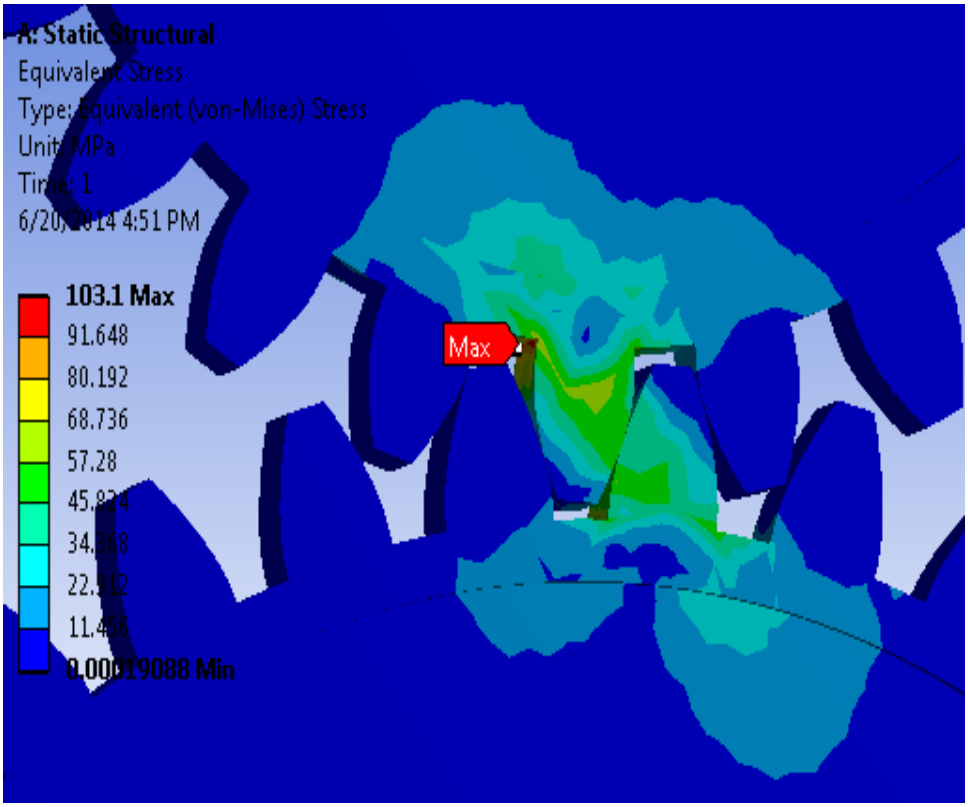

Fig. 5.3 Three dimensional equivalent von-Mises stress (bending) in upper and idler gear assembly after modifications

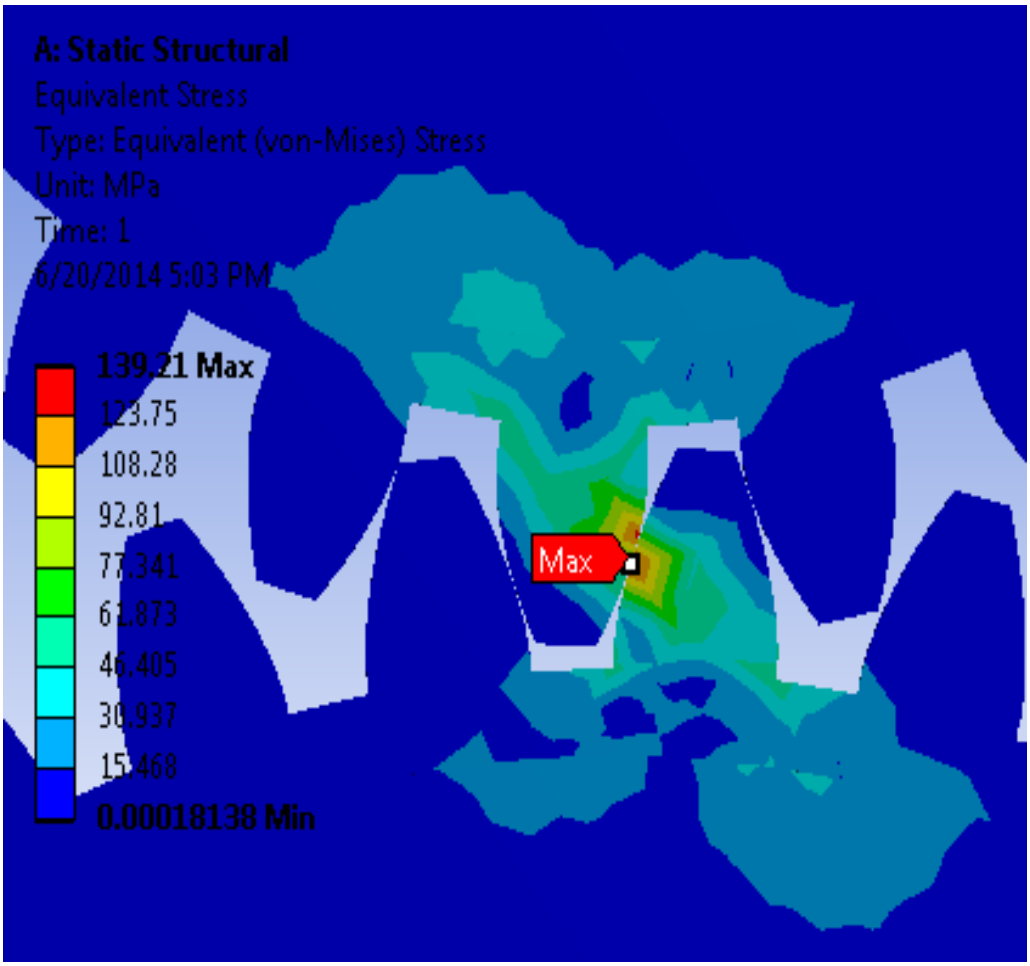

Fig. 5.4 Three dimensional equivalent von Mises stress (contact) after modifications.

By conducting these analysis on remaining gears the following diameters values for the pocket are suggested.

Table 5.1 Size of pockets cut from different gears

Gear	Dia of Pocket	Depth
Upper gear	145 mm	5 mm
Idler gear	215.5 mm	5 mm
Lower gear	152 mm	5 mm

5.3 Modal analysis after modifications

5.3.1 Mode shapes in free stress state and single pair tooth contact after modifications.

After modifications of gears the same procedure as mentioned earlier is adopted to determine the first six mode shapes subjected to single pair tooth contact in free stress state.

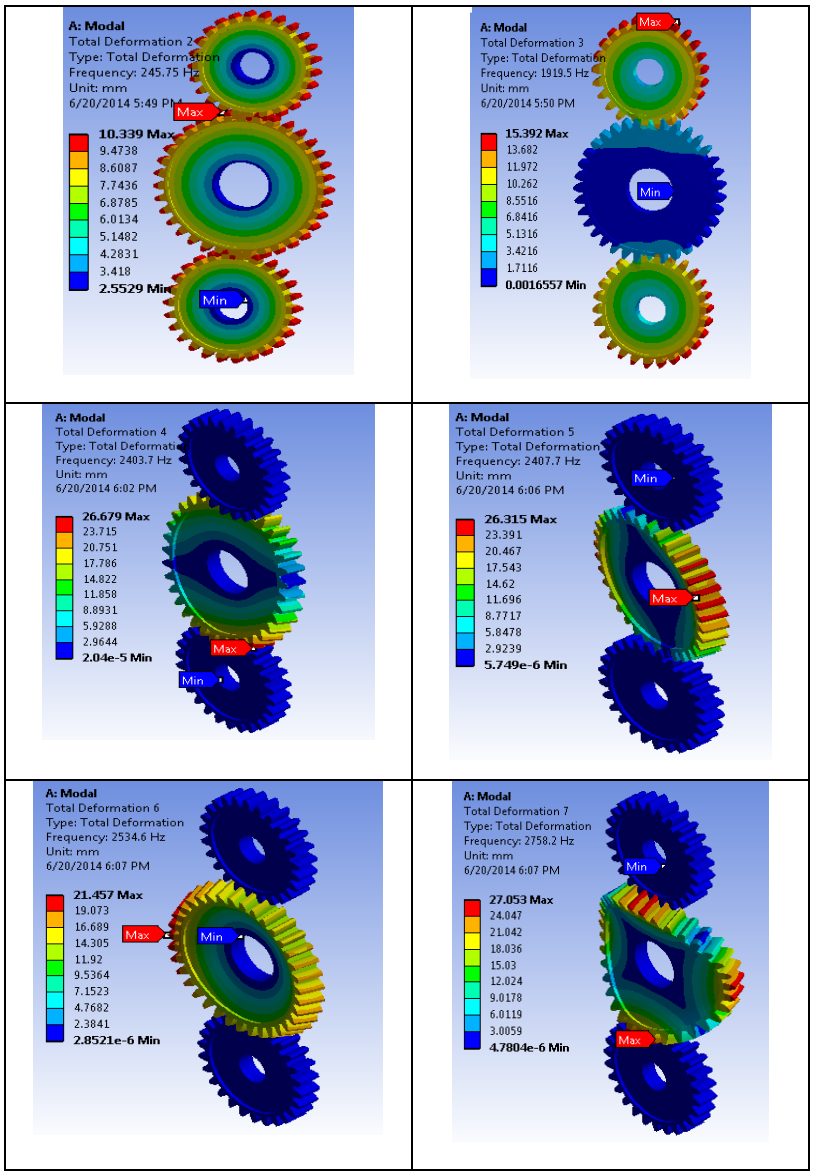

Fig. 5.5 First six mode shapes of the gear train in free stress state and single pair tooth contact after modifications.

Natural frequencies

Fig. 5.6 shows natural frequencies obtained.

	Mode	Frequency [Hz]
1	1.	245.75
2	2.	1919.5
3	3.	2403.7
4	4.	2407.7
5	5.	2534.6
6	6.	2758.2

Fig. 5.6 First six natural frequencies in free stress state and single pair tooth contact after modifications.

5.3.2 Mode shapes in pre-stress state and single pair tooth contact after modifications.

In pre stress state same procedure is adopted as mentioned in previous FE model.

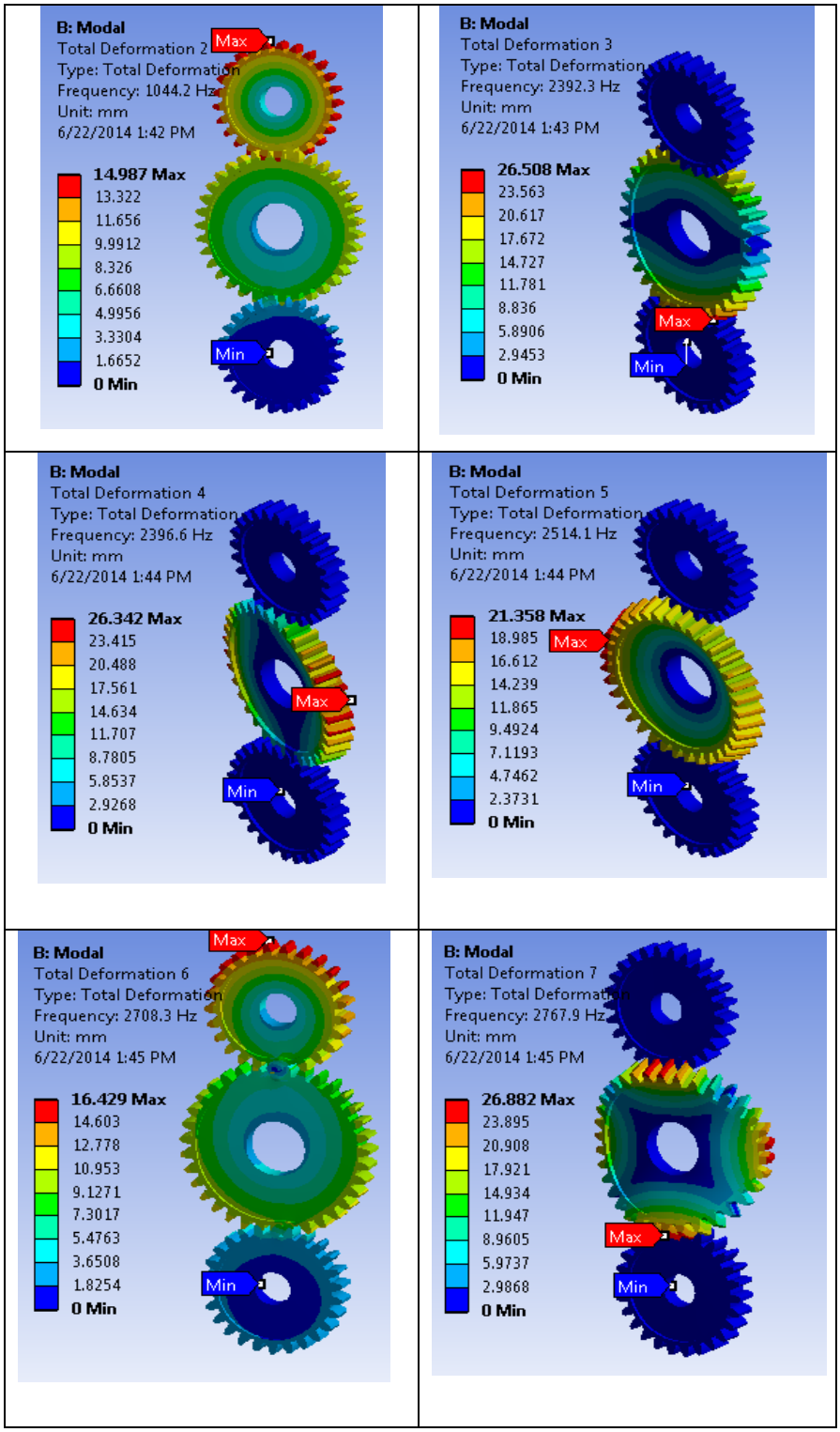

Fig. 5.7 First six mode shapes of the gear train in pre-stress state and single pair tooth contact after modifications.

Natural frequencies

Natural frequencies are obtained as shown in fig. 5.8

	Mode	Frequency [Hz]
1	1.	1044.2
2	2.	2392.3
3	3.	2396.6
4	4.	2514.1
5	5.	2708.3
6	6.	2767.9

Fig.5.8 First six natural frequencies in pre-stress state and single pair tooth contact after modifications

It is found that natural frequencies obtained after modification from FE analysis is low as 245 HZ, and it is much higher from operating frequency range of a gear train of a rotavator, so gear train is working under safe conditions.

6.1 Conclusion

In this work the bending stress and contact stress analysis on rotavator gears are performed using the finite element analysis software and obtained results are compared with exact mathematical models. The FEA bending stress results obtained are compared with results obtained from Lewis bending stress equation and results are in good agreement with the difference of 1.6%. The contact stress results obtained from FEA are compared with values calculated from Hertz contact stress equation, and results are in good agreement with the difference of 5.37%. The maximum bending stress occurs at root fillet of the input gear.

Modal analysis on spur gear train is studied using FEA under pre-stress state and free-stress state and mode shapes and natural frequencies are calculated while the gear train subjected to single pair tooth contact and double pair tooth contact. Lowest natural frequency is compared with operating frequency range of gear train of a rotavator, and found that operating frequency range is 3.75 Hz to 4.5 Hz which is much low as compare to lowest natural frequency i.e. 229 HZ.

The FE models are also used to study the effect of change in size of stress relieving feature.

6.2 Future scope

1. These types of analysis can be performed on first gear box of rotavator (i.e. sun and planet gears).

2. This work can be further extended considering the effect of shaft deflection on spur gear train.

3. Dynamic analysis can also be performed.

References

[1]. Jong Boon Ooi, Xin Wang, ChingSeong Tan, Jee-Hou Ho and Ying Pio Lim. Modal and stress analysis of gear train design in portal axle using finite element modeling and simulation. Mechanical Science and Technology; 2012, 26 (2): 575-589.

[2]. Mehmet Topakci, H.kursat Celik, Deniz Yilmaz and Ibrahim Akinci. Stress analysis on transmission gears of a rotary tiller using finite element method. Akdeniz university ziraat fakultesi dergisi; 2008, 21(2): 155-160.

[3]. Ali Raad Hassan. Contact stress analysis of spur gear teeth pair. World Academy of Science, Engineering and Technology; 2009, 3: 10-20.

[4]. Shreyash D Patel. Finite element analysis of stresses in involute spur and helical gear. Master of science Thesis; 2010, University of Texas.

[5]. Shuting Li. Finite element analyses for contact strength and bending strength of a pair of spur gears with machining errors, assembly errors and tooth modifications. Mechanism and Machine Theory; 2007, 42: 88–114.

[6]. Ignacio Gonzalez-Perez, Jose L Iserte and Alfonso Fuentes. Implementation of Hertz theory and validation of a finite element model for stress analysis of gear drives with localized bearing contact. Mechanism and Machine Theory; 2011, 46: 765–783.

[7]. Shuting Li. Effect of addendum on contact strength, bending strength and basic performance parameters of a pair of spur gears. Mechanism and Machine Theory; 2008, 43: 1557–1584.

[8]. Zaigang Chen and Yimin Shao. Mesh stiffness calculation of a spur gear pair with tooth profile modification and tooth root crack. Mechanism and Machine Theory; 2013, 62: 63–74.

[9]. Miryam B Sánchez, Jose I. Pedrero and Miguel Pleguezuelos. Critical stress and load conditions for bending calculations of involute spur and helical gears. International Journal of Fatigue; 2013, 48: 28–38.

[10]. J. Kramberger, M. Sraml, S. Glodez, J. Flasker and I. Potrc. Computational model for the analysis of bending fatigue in gears. Computers and Structures; 2004, 82: 2261–2269.

[11]. K. Mao. Gear tooth contact analysis and its application in the reduction of fatigue wear. Wear; 2007, 262: 1281–1288.

[12]. Juha Hedlund and Arto Lehtovaara. Modeling of helical gear contact with tooth deflection. Tribology International; 2007, 40: 613–619.

[13]. Yi-Cheng Chen and Chung-Biau Tsay. Stress analysis of a helical gear set with localized bearing contact. Finite Elements in Analysis and Design; 2002, 38: 707–723.

[14]. Shuting Li. Experimental investigation and FEM analysis of resonance frequency behavior of three-dimensional, thin-walled spur gears with a power-circulating test rig. Mechanism and Machine Theory; 2008, 43: 934–963.

[15]. Tengjiao Lin, H. Ou and Runfang Li. A finite element method for 3D static and dynamic Contact, impact analysis of gear drives. Comput. Methods Appl. Mech. Engrg.; 2007, 196: 1716–1728.

[16]. S.P Shinde, A.A Nikam and T.S Mulla. Static analysis of spur gear using finite element analysis. IOSR Journal of Mechanical and Civil Engineering; 2012, 26-31.

[17]. Kadir Cavdar, Fatih Karpat and Fatih C. Babalik. Computer Aided Analysis of Bending Strength of Involute Spur Gears with Asymmetric Profile. Journal of Mechanical Design; 2005, 127: 477-484.

[18]. Alexander L. Kapelevich and Yuriy V. Shekhtman. Direct Gear Design: Bending Stress Minimization. Gear Technology; 2003.

[19]. G. Mallesh, VB Math, Venkatesh, H J Shankarmurthy, Shiva Prasad P and K Aravinda. Parametric analysis of Asymmetric Spur Gear Tooth. Machines and Mechanisms; 2009, 398-403.

[20]. Ram Krishna Rathore and Abhishek Tiwari. Bending stress analysis and optimization of spur gear. International Journal of Engineering Research & Technology; 2014, 3: 2044-2049.

[21]. Ag power. (n.d.). *Ag power: New products of john-deere.* Retrieved May 10, 2014, from http://www.ag-power.com/new-product/new-products/john-deere

[22]. Shodhganga. (n.d).*shodhganga: Mechanical properties of Steel grade EN-353.* Retrieved Feb 12, 2014 from https://www.google.co.in/#q=mechanical+properties+of+steel+grade+EN353

[23]. http://www.google.co.in/images